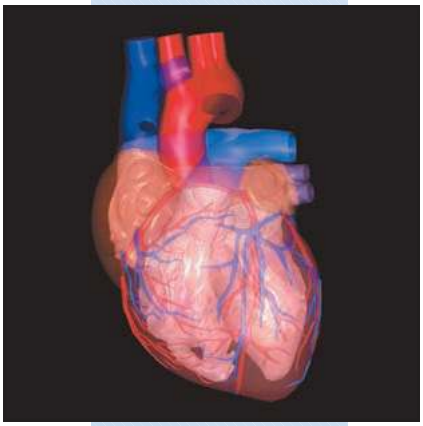



# The Principles of Software QRS Detection

## *Reviewing and Comparing Algorithms for Detecting this Important ECG Waveform*

**Bert-Uwe Köhler, Carsten Hennig, Reinhold Orglmeister**
Department of Electrical Engineering,
Biomedical Electronics Group,
Berlin University of Technology

The QRS complex is the most striking waveform within the electrocardiogram (ECG). Since it reflects the electrical activity within the heart during the ventricular contraction, the time of its occurrence as well as its shape provide much information about the current state of the heart. Due to its characteristic shape (see Fig. 1) it serves as the basis for the automated determination of the heart rate, as an entry point for classification schemes of the cardiac cycle, and often it is also used in ECG data compression algorithms. In that sense, QRS detection provides the fundamentals for almost all automated ECG analysis algorithms.

Software QRS detection has been a research topic for more than 30 years. The evolution of these algorithms clearly reflects the great advances in computer technology. Whereas in the early years the computational load determined the complexity and therefore the performance of the algorithms, nowadays the detection performance is the major development objective. The computational load becomes less and less important. The only exception from this trend is probably the development of QRS detection algorithms for battery-driven devices.

Within the last decade many new approaches to QRS detection have been proposed; for example, algorithms from the field of artificial neural networks [47, 105, 119, 122], genetic algorithms [91], wavelet transforms, filter banks [2, 54, 66] as well as heuristic methods mostly based on nonlinear transforms [59, 107, 114]. It is the intention of the authors to provide an overview of these recent developments as well as of formerly proposed algorithms that were already reviewed in [34, 51, 84]. The overview is focused on the description of the *principles*. Algorithmic details can be found in the original papers that are referenced at the end of this article.

Beyond QRS detection, many papers have been published in related fields; e.g., ECG signal enhancement [15, 17, 23, 28, 90, 99] or pattern classification [8, 26, 31, 40, 62, 63, 70, 71, 72, 108, 113, 119]. The algorithms described in these papers are not the topic of this article. However, although not directly applied to QRS detection, many of these algorithms may be useful in processing stages prior to QRS detection.

### Overview

The rapid development of powerful microcomputers promoted the widespread application of software QRS detection algorithms in cardiological devices. Beginning about 30 years ago, software QRS detection has replaced more and more hardware QRS detectors.

Already in the early years of automated QRS detection, an algorithmic structure was developed that is now shared by many algorithms. As shown in Fig. 2 it is divided into a preprocessing or feature extraction stage including linear and nonlinear filtering and a decision stage including peak detection and decision logic. Often an extra processing block is used for the exact determination of the temporal location of the assumed QRS candidate. In this article the different algorithms are discriminated with respect to their preprocessing stages, because most of the decision stages are rather heuristic and dependent on the preprocessing results.

### Approaches Based on Signal Derivatives and Digital Filters

Typical frequency components of a QRS complex range from about 10 Hz to about 25 Hz. Therefore, almost all QRS detection algorithms use a filter stage prior to

 0739-5175/02/$17.00©2002IEEE 

the actual detection in order to attenuate other signal components and artifacts, such as P-wave, T-wave, baseline drift, and incoupling noise. Whereas the attenuation of the P- and T-wave as well as baseline drift requires high-pass filtering, the suppression of incoupling noise is usually accomplished by a low-pass filter. The combination of low and high pass means effectively the application of a bandpass filter, in this case with cut-off frequencies at about 10 Hz and 25 Hz.

In many algorithms, high- and low-pass filtering are carried out separately. Some algorithms, such as [3, 7, 33, 38, 45, 78, 83], use only the high-pass filter part. The filtered signals are then used for the generation of a feature signal in which the occurrence of a QRS complex is detected by comparing the feature against fixed or adaptive thresholds. Almost all algorithms use additional decision rules for the reduction of false-positive detections.

### Derivative-Based Algorithms

The high-pass filter is often, in particular in the older algorithms, realized as a differentiator. This points out the usage of the characteristic steep slope of the QRS complex for its detection. Difference equations of possible differentiator filters are [3, 7, 33, 38, 45, 78, 83]

$$y_1(n) = x(n+1) - x(n-1) \tag{1}$$

$$y_1(n) = 2x(n+2) + x(n+1) - x(n-1) - 2x(n-2) \tag{2}$$

$$y_1(n) = x(n) - x(n-1) \tag{3}$$

$$y_1(n) = \tilde{x}(n) - \tilde{x}(n-1) \tag{4}$$

where

$$\tilde{x}(n) = \begin{cases} |x(n)| & |x(n)| \geq \Theta \\ \Theta & |x(n)| < \Theta. \end{cases} \tag{5}$$

and $\Theta$ is an amplitude threshold determined from the measured ECG signal $x(n)$. In most cases, the differentiator from Eq. (1) is used. Some algorithms also compute the second derivative. It can be estimated by [3, 7]

$$y_2(n) = x(n+2) - 2x(n) + x(n-2). \tag{6}$$

Typical features $z(n)$ of such algorithms are the differentiated signal itself [33, 38, 78]

$$z(n) = y_1(n), \tag{7}$$

a linear combination of the magnitudes of the first and the second derivative [7]

$$z(n) = 1.3|y_1(n)| + 1.1|y_2(n)|, \tag{8}$$

or a linear combination of the smoothed first derivative magnitude and the magnitude of the second derivative [3]

$$z(n) = \tilde{y}_1(n) + |y_2(n)| \tag{9}$$

where $\tilde{y}_1(n) = \{0.25, 0.5, 0.25\} * |y_1(n)|$ and * denotes the linear convolution operator.

The detection of a QRS complex is accomplished by comparing the feature against a threshold. Usually the threshold levels are computed signal dependent such that an adaption to changing signal characteristics is possible. For the feature in Eq. (7), the threshold [33, 38, 78]

$$\Theta_x = 0.3 \ldots 0.4 \cdot \max[x] \tag{10}$$

is proposed, where the maximum is determined online or from the current signal segment. Most QRS detectors use this or a similar method to determine the threshold.

The peak detection logic is frequently completed by further decision rules that are applied in order to reduce the number of false-positive detections. Such rules usually put heuristically found constraints on the timing and the sign of the features or introduce secondary thresholds to exclude non-QRS segments of the ECG with QRS-like feature values [3, 7, 33, 38, 45, 78, 81, 103].

### Algorithms Based on Digital Filters

Algorithms based on more sophisticated digital filters were published in [12, 26, 29, 30, 41, 55, 65, 67, 81, 83, 85, 101, 106, 107, 123].

In [83] an algorithm is proposed where the ECG is filtered in parallel by two different low-pass filters with different cut-off frequencies. The difference between the filter outputs is effectively the bandpass filtered ECG $y_1(n)$, which is afterwards further processed by

$$y_2(n) = y_1(n) \left[ \sum_{k=-m}^{m} y_1^2(n+k) \right]^2. \tag{11}$$

This nonlinear operation leads to a relative suppression of small values and a slight smoothing of the peaks. The feature signal $z(n)$ is formed out of $y_2(n)$ by putting additional sign constraints on the output signal of the low pass with the higher cut-off frequency. The threshold is computed adaptively by $\Theta = \max[z(n)] / 8$.

In [106] and [107] the MOBD (multiplication of backward difference) algorithm is proposed. It is essentially an

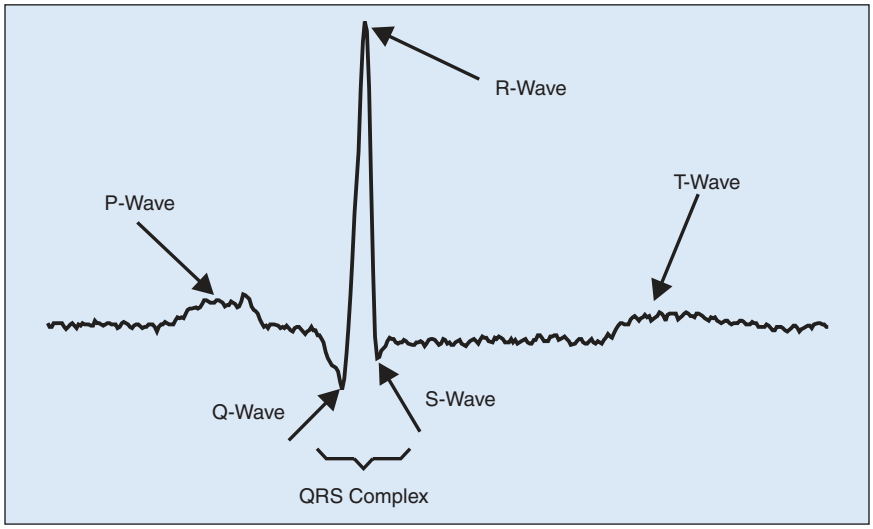


**1. The QRS complex within the ECG signal.**

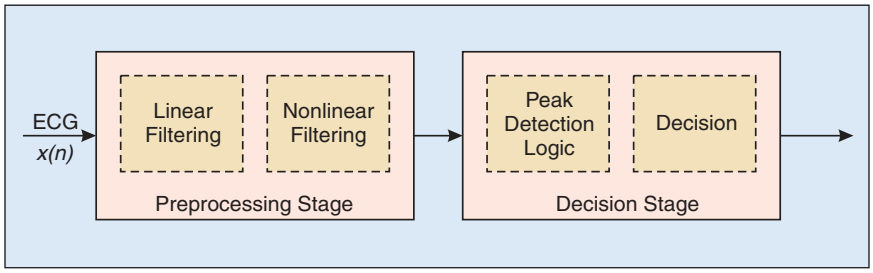


**2. Common structure of the QRS detectors.**

**The detection of a QRS complex is accomplished by comparing the feature against a threshold.**

*AND*-combination of adjacent magnitude values of the derivative. The MOBD of the order $N$ is then defined by

$$z(n) = \prod_{k=0}^{N-1} |x(n-k) - x(n-k-1)|. \quad (12)$$

In order to avoid a high feature signal during noisy segments, an additional sign consistency constraint is imposed; i.e.,

$$z(n) = 0 \quad \text{if } \text{sign}[x(n-k)] \neq \text{sign}[x(n-k-1)], \quad (13)$$

where $k = 0,1,\ldots,N-2$. A proposed value for the order of MOBD is $N = 4$ [107]. The threshold $\Theta$ is set to the feature maximum $z_{\max}$ after the refractory period and then halved whenever a fixed time period is elapsed. The threshold is bounded by a lower limit that is also adaptive.

The algorithms described in [41] and [85] use basically the same preprocessor. The ECG is bandpass filtered and afterwards differentiated. The feature signal $z(n)$ is computed by squaring and averaging the output of the differentiator. The bandpass and differentiator use filter coefficients that are particularly suited for an implementation on fixed-point processors with a short word length. For the peak detection, a variable $v$ is introduced that contains the value of the most recent feature maximum. Peaks in the feature signal are detected by comparing the feature against $v$. If the feature drops below $v/2$ a peak is detected. Then the current value of $v$ is taken as the peak height and $v$ is reset to the current value of the feature signal; i.e., $v = z(n)$. The principle of the peak detection is shown in Fig. 3. The fiducial mark is set to the location of the largest peak in the bandpass-filtered signal in an interval from 225 ms to 125 ms preceding a peak detection. The fiducial mark and the height of the peak are put into an event vector that is further processed by the decision stage. In the decision stage, a QRS peak level $L_P$ and a noise level $L_N$ are estimated recursively by

$$L_P(n) = \lambda_P \cdot L_P(n-1) + (1-\lambda_P) \cdot A_P \quad (14)$$

$$L_N(n) = \lambda_N \cdot L_N(n-1) + (1-\lambda_N) \cdot A_P, \quad (15)$$

where $\lambda_N$ and $\lambda_P$ are forgetting factors (e.g., $\lambda \approx 0.98$) and $A_P$ is the peak amplitude. Depending on whether a peak is classified as QRS complex or as a noise peak, either the QRS peak level $L_P$ *or* the noise level $L_N$ is updated using Eq. (14) or Eq. (15), respectively. Eventually, the detection threshold is determined from

$$\Theta = L_N + \tau \cdot (L_P - L_N), \quad (16)$$

where the positive threshold coefficient $\tau < 1$ is a design parameter.

In [67] the feature signal $z(n)$ is computed in a way similar to [41] and [85] but using different filters. In contrast to [41] and [85], the feature signal is divided into segments of 15 points. The maximum of each segment is compared to an adaptive noise level and an adaptive peak level estimate and classified depending on the distance to each of the estimates. The fiducial point of the QRS complex is set to the location within the QRS segment where the maximum of the ECG and a zero crossing in its first derivative occur at the same time.

Although [26] describes an ECG waveform detection by neural networks, the QRS detection is accomplished using a feature extractor based on digital filtering. The feature signal $z(n)$ is generated by filtering the ECG with two different bandpass filters and afterwards multiplying the filter outputs $w(n)$ and $f(n)$; i.e.,

$$z(n) = w(n) \cdot f(n). \quad (17)$$

This procedure is based on the assumption that a QRS complex is characterized by simultaneously occurring frequency components within the passbands of the two bandpass filters. The multiplication operation performs the *AND*-combination. That is, only if both filter outputs are high then the feature is high and indicates a QRS complex. The location of the maximum amplitude in the feature is taken as the location of the R-wave.

The use of recursive and nonrecursive median filters, i.e.

$$y(n) = \text{median}[y(n-m),\ldots,y(n-1), x(n),x(n+1),\ldots,x(n+m)] \text{ and} \quad (18)$$

$$y(n) = \text{median}[x(n-m),\ldots,x(n-1), x(n),x(n+1),\ldots,x(n+m)], \quad (19)$$

is proposed, for example, in [123]. The *median* operator applied to a vector $\mathbf{x} = [x_1,\ldots,x_N]$ means sorting the elements of the vector according to their values and then taking the midpoint $y = \mathbf{x}_{\text{sorted}}(N/2)$ as the filter output. In [123] a combination of two median filters and one smoothing filter is used to form a bandpass filter. The additional signal processing steps are similar to [41, 85].

Generalized digital filters for ECG processing with the transfer function

$$H(z) = (1-z^{-K})(1+z^{-1})^L \quad K, L > 0 \quad (20)$$

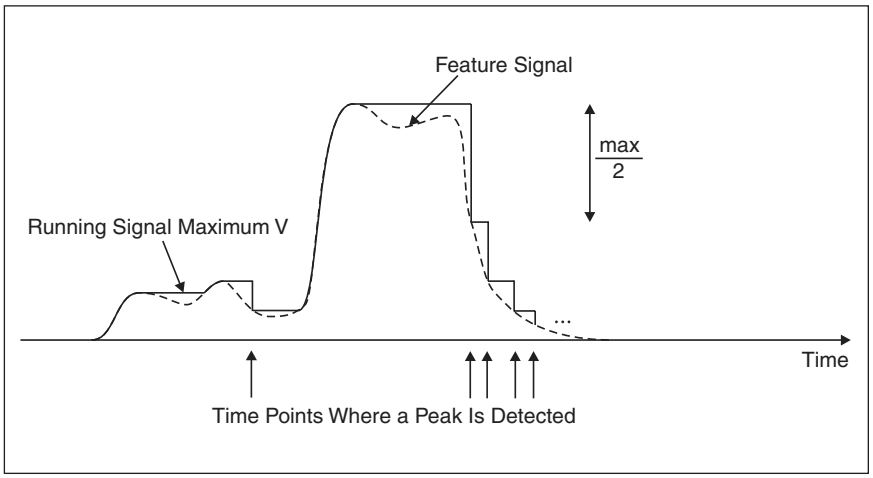


**3. Peak detector proposed in [41].**

are proposed in [12, 100]. Such filters have a linear phase response and are computationally highly efficient. They were applied, for example, in [101] where $(K,L)=(1,2)$ at a sampling rate $f_T=100$ Hz and in [29] where $(K,L)=(5,4)$ at a sampling frequency $f_T=250$ Hz. Other reported applications of these filters can be found in [30, 81].

Digital filters have been widely applied to QRS detection. However, having described the major principles, we conclude this section here. Further articles on filter-based QRS detection methods include [5, 32, 48, 55, 58, 65, 79, 110, 111, 112, 102, 121].

## Wavelet-Based QRS Detection

### Wavelet Transform and Singularity Detection

The wavelet transform (WT) of a function $f(t)$ is an integral transform defined by

$$Wf(a,b)=\int_{-\infty}^{\infty} f(t)\psi^*_{a,b}(t)dt. \tag{21}$$

where $\psi^*(t)$ denotes the complex conjugate of the wavelet function $\psi(t)$. The transform yields a *time-scale* representation similar to the *time-frequency* representation of the short-time Fourier transform (STFT). In contrast to the STFT, the WT uses a set of analyzing functions that allows a variable time and frequency resolution for different frequency bands. The set of analyzing functions, the wavelet family $\psi_{a,b}$, is deduced from a *mother wavelet* $\psi(t)$ by

$$\psi_{a,b}(t)=\frac{1}{\sqrt{2}}\cdot\psi\left(\frac{t-b}{a}\right) \tag{22}$$

where $a$ and $b$ are the *dilation* (scale) and *translation* parameter, respectively. The scale parameter $a$ of the WT is comparable to the frequency parameter of the STFT. The mother wavelet is a short oscillation with zero mean. An example is depicted in Fig. 4.

The discrete wavelet transform (DWT) results from discretized scale and translation parameters; e.g., $a=2^j$ and $b=n\cdot 2^j$ where $j$ and $n$ are integer numbers. This choice of $a$ and $b$ leads to the dyadic DWT (DyWT)

$$Wf(2^j,b)=\int_{-\infty}^{\infty} f(t)\cdot\psi^*_{2^j,b}(t)dt \tag{23}$$

with

$$\psi_{2^j,b}(t)=\frac{1}{2^{j/2}}\cdot\psi\left(\frac{t-b}{2^j}\right)=\frac{1}{2^{j/2}}\cdot\psi\left(\frac{t}{2^j}-n\right)$$

and

$$j,n\in\mathbf{Z}. \tag{24}$$

Although defined as an integral transform, the DyWT is usually implemented using a dyadic filter bank where the filter coefficients are directly derived from the wavelet function used in the analysis [14,104]. The input signal to the filter bank is the sampled ECG signal.

Except for [2] and [39] all wavelet-based peak detection methods mentioned in this review [6, 24, 54, 66, 93] are based on Mallat's and Hwang's approach for singularity detection and classification using local maxima of the wavelet coefficient signals [74]. Therein the correspondence between singularities of a function $f(t)$ and local maxima in its wavelet transform $Wf(a,t)$ is investigated. It is shown that singularities correspond to pairs of modulus maxima across several scales (see Fig. 12). Figure 5 clarifies the correspondence between a signal with singularities and its wavelet coefficients. Peak classification is accomplished by the computation of the singularity degree (peakiness); i.e., the local Lipschitz regularity $\alpha$, which is estimated from the decay of the wavelet coefficients by [74]

$$\alpha_j=\log_2\left|Wf(2^{j+1},n^{j+1})\right|-\log_2\left|Wf(2^j,n^j)\right| \tag{25}$$

and

$$\alpha=\frac{\alpha_1+\alpha_2}{2}. \tag{26}$$

### Singularity Detection-Based Approaches

The algorithm proposed by Mallat and Hwang [74] was first applied to QRS detection in [66]. R-peaks are found by scanning for simultaneous modulus maxima in the relevant scales of the WT. For a valid R-peak the estimated Lipschitz regularity must be greater than zero; i.e., $\alpha>0$ [66]. Besides the condition on the Lipschitz regularity, the algorithm in [66] applies further heuristic decision rules such as conditions on the sign and the timing of the peak occurrence within the different scales.

The methods in [6] and [50] are directly derived from [66]. Although both detection methods are extensively simplified compared to the original algorithm, the reported results are still very good. Descriptions of two implementations of the algorithm from [66] on digital signal processors can be found in [57] and [95].

Further QRS detection algorithms based on local maxima are presented in [24], [93], and [54]. In [24], characteristic points are detected by comparing the coefficients of the discrete WT on selected scales against fixed thresholds. The algorithm described in [93] divides the ECG into segments of a fixed length. R-peaks are detected when the locations of modulus maxima of adjacent scales

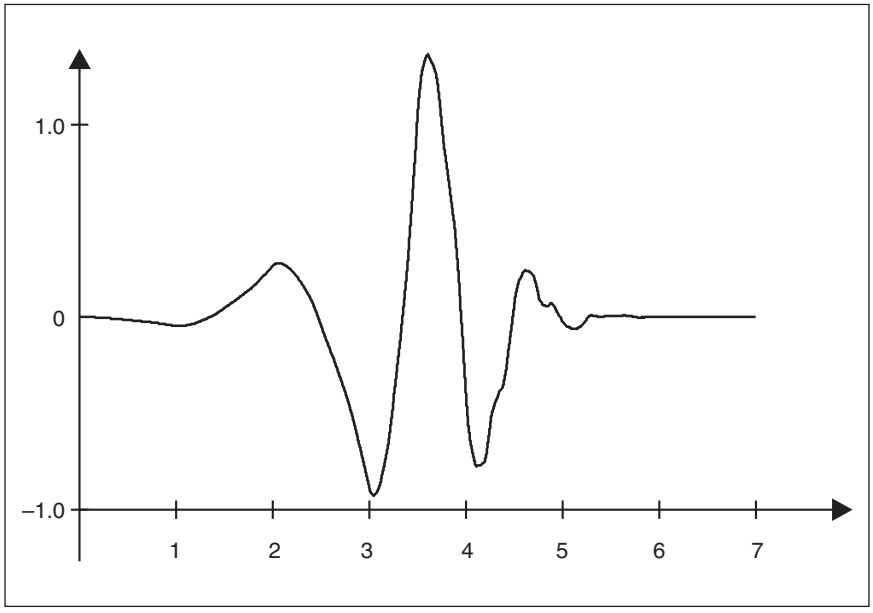


**4. Example of a wavelet function (Daubechies-4 wavelet).**

exceed a threshold that is calculated for every segment.

In [39], the wavelet-based zero crossing representation from [73] is used for pattern recognition. This pattern recognition method consists of a learning and a recognition phase. In the learning phase, a set of generalized feature vectors is generated from a set of example patterns, using the zero crossing representation of the example. In the recognition phase, the feature vectors are computed for fixed-length segments of the ECG and compared against the generalized feature vectors. If a percentage match criterion exceeds the threshold, an R-peak is detected.

### Filter-Bank Methods

Filter banks are closely related to wavelets. Their application to QRS detection is reported in [2]. Therein a 32-band filter bank is used to generate downsampled subband signals. Similar to [26], it is assumed that the QRS complex is characterized by a simultaneous occurrence of ECG frequency components in the subbands $w_l, l = 1, \ldots, 4$. From these subbands three features, $p_1, p_2$, and $p_3$, are derived; i.e.,

$$p_1(n) = \sum_{l=1}^{3} |w_l(n)| \tag{27}$$

$$p_2(n) = \sum_{l=1}^{4} |w_l(n)| \tag{28}$$

$$p_3(n) = \sum_{l=2}^{4} |w_l(n)|. \tag{29}$$

Finally, the actual QRS detection is accomplished by a sophisticated combination of the features in the following five-stage detection logic.

### Related Methods

The wavelet transform has also been used for classification; e.g., in [16, 21, 56, 96]. In [116] the WT was applied to the detection of ventricular late potentials (VLPs) in manually segmented ECG signals. The authors of [21] give a brief survey of the continuous WT (CWT) of ECG and heart rate variability (HRV) signals and demonstrate the possibility of data compression by thresholding of wavelet coefficients. In [16] the application of the CWT to ECG signals of healthy subjects and patients with cardiac diseases is reported and compared to the short-time Fourier transform. In [56] energy parameters are derived from the CWT to discriminate between normal sine rhythm and cardiac arrythmias like ventricular fibrillation, ventricular tachycardia, and atrial fibrillation.

Wavelet-based filtering and noise reduction methods with applications to ECG signal processing are published in [49, 60] and [77].

## Neural Network Approaches

### Neural Networks

Artificial neural networks have been widely applied in nonlinear signal processing, classification, and optimization. In many applications their performance was shown to be superior to classical linear approaches.

In ECG signal processing, mostly the multilayer perceptron (MLP), radial basis function (RBF) networks, and learning vector quantization (LVQ) networks are used. As depicted in Fig. 6, the MLP network consists of several layers of interconnected neurons where each neuron represents a processing function

$$y = f\left( w_0 + \sum_{i=1}^{N} w_i \mathrm{x}_i \right) \tag{30}$$

with $w_i$ as the weight assigned to input $x_i$ and $f(\cdot)$ as a linear or nonlinear function. In the nonlinear case, $f(\cdot)$ is frequently defined as the logistic function $f(u) = 1/(1+e^{-u})$ or $f(u) = \tanh(u)$. RBF networks are an implementation of the functional

$$y(n) = \sum_{i=1}^{N} w_i \exp\left( -\frac{\mathbf{x}(n) - \mathbf{c}_i}{\sigma_i} \right) \tag{31}$$

where $\mathbf{x}(n)$ denotes some input data vector. The number $N$ of neurons, the coefficients $w_i$, the center vectors $\mathbf{c}_i$, and the standard deviations $\sigma_i$ are the parameters of the network. The exponentials may also be replaced by other functions; e.g., wavelets. RBF networks are closely related to fuzzy logic methods [13]. The advantage of RBF networks over MLP networks is, similar to fuzzy-logic methods, the possibility to interpret the parameters. This makes the results more predictable and hence reliable.

The LVQ network consists of an input layer, a competitive layer, and a linear layer. The competitive layer automatically learns to classify input vectors into subclasses, where the maximum number of subclasses $N$ equals the number of competitive neurons. In this layer, a classification is accomplished on the basis of the Euclidian distance between the input vector and the weight vector of each of the competitive neurons. Finally, the linear layer combines the subclasses of the first layer to the user-defined target classes. The structure of the LVQ network is shown in Fig. 7.

In order to accomplish the application-dependent task (e.g. approximation or classification), the parameters of the network need to be trained. Whereas the MLP and RBF networks are trained by supervised learning algorithms, the LVQ network is adjusted in an unsupervised manner. Appropriate training algorithms are described in the literature; for example, in [11, 44].

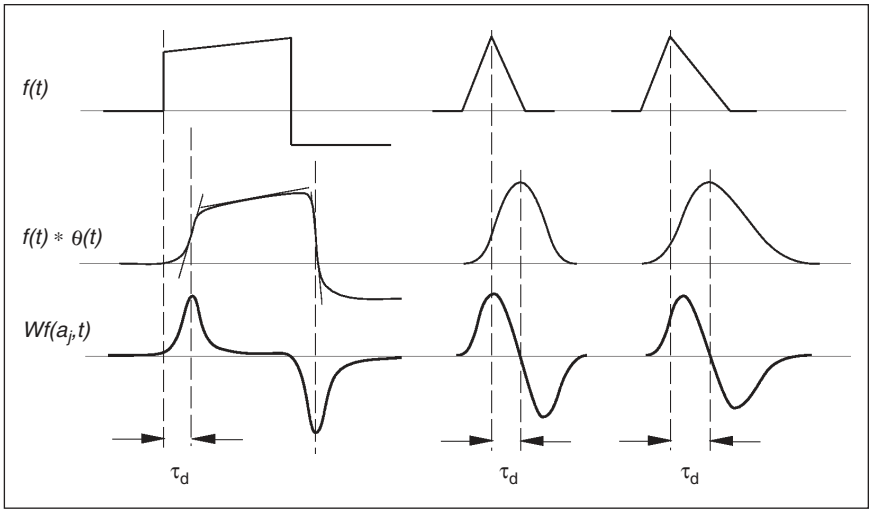


**5. Example of the correspondence between singularities of a function $f(t)$ and local maxima in its wavelet transform $Wf(a,t)$. The mother wavelet is the derivative of a smoothing function $\theta(t)$.**

The application of neural networks in the field of ECG waveform classification is reported in [8, 26, 31, 40, 47, 62, 63, 70, 71, 72, 105, 108, 113, 119, 122]. Some of these algorithms [47, 105, 119, 122], are also concerned with the QRS detection problem.

### Neural Networks as Adaptive Nonlinear Predictors

In the context of QRS detection, neural networks have been used as adaptive nonlinear predictors [47, 119, 122]. The objective is to predict the current signal value $x(n)$ from its past values $x(n-i)$, $i > 0$.

Because the ECG consists almost solely of non-QRS segments, the neural network converges to a point where samples from non-QRS segments are well predicted. Segments with sudden changes (i.e., QRS segments) follow a different statistics and lead to a sudden increase in the prediction error. It follows that the prediction error $e(n)$ can be used as a feature signal for QRS detection.

Due to the nonlinear behavior of the background noise as described in [122], a nonlinear prediction filter may show better performance than its linear counterpart. In [122, 47, 119] the neural network is an MLP network with a three-layer structure. The input layer consists of eight to ten linear neurons with the time-delayed signal samples as inputs; the hidden layer has three to five nonlinear (logistic nonlinearity) neurons and the output layer contains one, again a linear neuron. In [119] the network is trained prior to the detection on carefully selected samples. In contrast to prior learning in [122] the network is trained online and hence able to adopt to changing signal statistics. In [122] the output of the nonlinear prediction filter is further processed by a matched filter, providing a better attenuation of the residual noise.

### Learning Vector Quantization for QRS Detection

In [105] the authors propose the application of a two-layer LVQ network for QRS detection and the discrimination of premature ventricular contractions (PVC). The input and the competitive layer consist of 20-40 neurons, whereas in the linear layer there are two neurons corresponding to the number of output classes. The input are adjacent samples of the ECG. Training data were taken from several records of the MIT/BIH database. The classification is carried out with an overlap of 10-30 samples. As reported in [105], the results do not reach the results of classical approaches, such as [85]. However, once trained the LVQ network offers fast computations and furthermore a discrimination between QRS and PVC contractions.

## Additional Approaches

### Adaptive Filters

The application of adaptive prediction filters to QRS detection has been investigated (e.g., in [61,42]). Figure 8 shows the structure of an FIR prediction filter. Similar to the nonlinear case (see the previous section) the objective of the filter is to gain an estimate $\hat{x}(n)$ for the current signal sample $x(n)$ from the past signal values by means of a weighted superposition; that is,

$$\hat{x}(n) = \sum_{i=1}^{P} a_i(n)x(n-i) \qquad (32)$$

with the time-variant coefficients $a_i(n)$, $i = 1 \ldots P$. They are adaptively adjusted according to the changing signal statistics. From the literature several adaption rules for the coefficients are known; e.g., the least mean square (LMS) algorithm

$$\mathbf{a}(n+1) = \mathbf{a}(n) + \lambda e(n)\mathbf{x}(n) \qquad (33)$$

where $\mathbf{a}(n) = [a_1(n), a_2(n), \ldots, a_P(n)]^T$ denotes the coefficient vector at time $n$, $\lambda$ is the step size parameter, $e(n) = x(n) - \hat{x}(n)$ denotes the prediction error, and $\mathbf{x}(n) = [x(n-1), x(n-2), x(n-2), \ldots, x(n-P)]^T$ is the vector of the time-delayed ECG signal samples. For a detailed description of the adaptive filtering methods, see [43].

The authors of [61] propose features on the basis of adaptive filtering. They suggest to use the differences between the coefficient vectors **a** at time $n$ and time $n-1$; i.e,

$$D(n) = \sum_{i=1}^{P} |a_i(n) - a_i(n-1)|^2, \qquad (34)$$

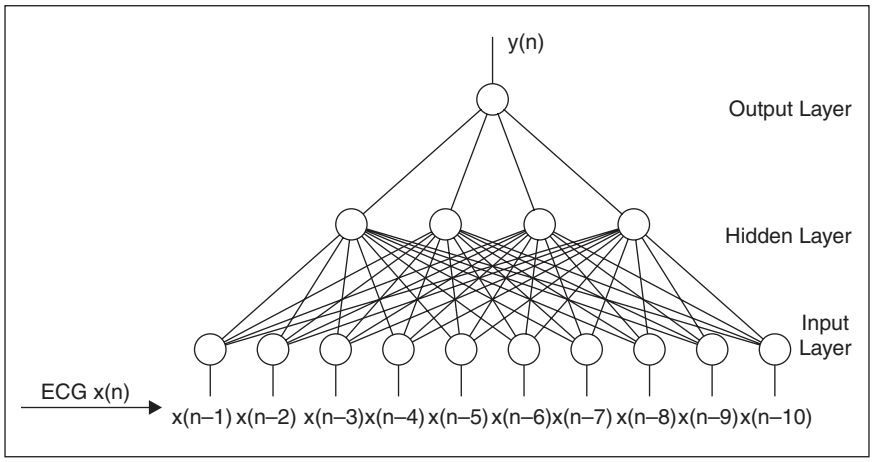


**6. Multilayer perceptron.**

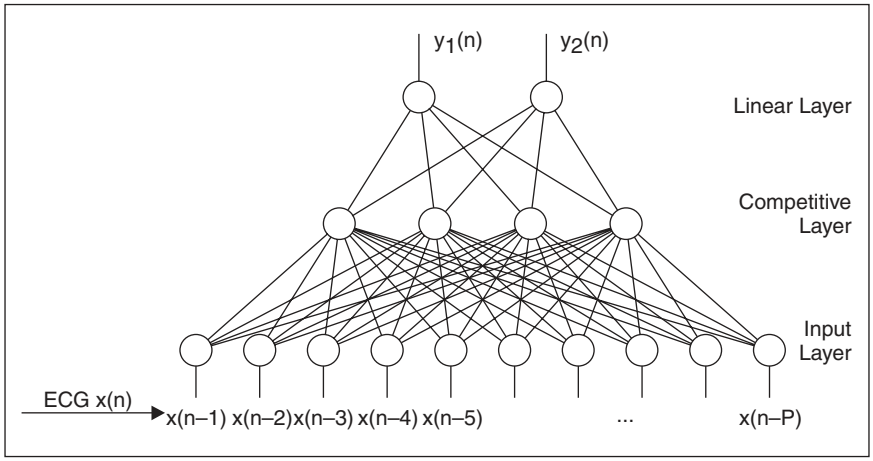


**7. LVQ network.**

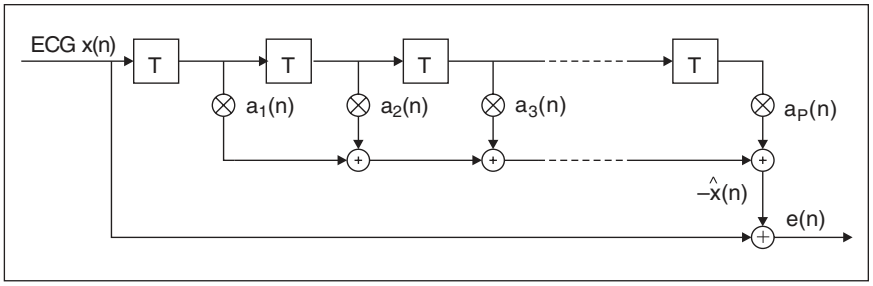


**8. Prediction filter.**

and a combination of the difference between the short time energies of the residual error of two consecutive segments

$$D_e(n) = \sum_{i=n}^{n+m} e^2(i) - \sum_{i=n-m}^{n} e^2(i). \quad (35)$$

Further applications of adaptive filters to QRS detection are reported in [68] and [22]. In [68] it was shown that at a sampling frequency of $f_T = 500$ Hz two tap filters are sufficient for a good prediction performance. In [22] the application of a midprediction filter

$$\hat{x}(n) = \sum_{k=-P}^{P} a_i x(n-i) \quad (36)$$

is proposed.

### Hidden Markov Models

In [20] the application of hidden Markov models (HMM) to QRS and ECG waveform detection is investigated. HMMs model the observed data sequence by a probability function that varies according to the state of an underlying (hidden) Markov chain. By means of the Markov chain the global structural characteristics of the process are preserved while the parameters of the probability density function account for the varying statistical properties of the observed data. The objective of the algorithm is to infer the underlying state sequence from the observed signal. In the case of ECG signals, possible states are P-wave, QRS, and T-wave. The advantage of this detection method is that not only the QRS complex is determined but also P- and T-waves. Problems of the method include a necessary manual segmentation for training prior to the analysis of a record, its patient dependence, and the considerable computational complexity even when the computationally efficient Viterby algorithm [20] is applied. For further details about HMMs, see e.g. [92,118].

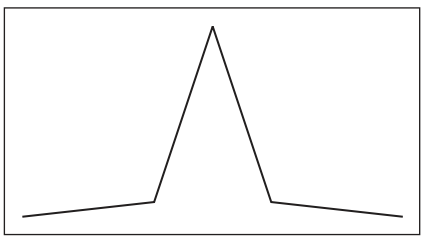

**9. Peaky structuring element for QRS detection.**

### Mathematical Morphology

The use of mathematical morphology operators for QRS detection was described in [114]. Mathematical morphology originates from image processing and was proposed for ECG signal enhancement in [18]. Therein the successful removal of impulsive noise from the ECG is reported.

Mathematical morphology is based on the terms *erosion* and *dilation*. Let $f: F \to I$ and $k: K \to I$ denote discrete functions, where the sets $F$ and $K$ are given by $F = \{0,1,\ldots,N-1\}$ and $K = \{0,1,\ldots,M-1\}$. $I$ is the set of integer numbers. The *erosion* of the function $f$ by the function $k$ is defined as [18]

$$(f \ominus k)(m) = \min_{n=0,\ldots,M-1} f(m+n) - k(n)$$
$$\text{for } N > M \text{ and } m = 0,\ldots,N-M \quad (37)$$

$k$ is also referred to as the *structuring element*. The values of $(f \ominus k)$ are always less than those of $f$.

The *dilation* of the function $f$ by the function $k$ is defined as [18]

$$(f \oplus k)(m) = \max_{n=0,\ldots,M-1} f(n) + k(m-n)$$
$$\text{for } N > M \text{ and } m = M-1,\ldots,N-1. \quad (38)$$

The values of $f \oplus k$ are always greater than those of $f$.

Erosion and dilation are combined for additional operations. *Opening*, denoted by °, is defined as erosion followed by a dilation. *Closing*, denoted by •, is defined as dilation followed by an erosion. Both operators manipulate signals in a comparable way. That is, to *open* a sequence $f$ with a flat structuring element $k$ will remove all peaks. To *close* the sequence with the same structuring element will remove all pits (negative peaks).

In [114], opening and closing operations are used for noise suppression as proposed in [18]; i.e.,

$$\tilde{x} = \frac{[(x \circ k) \bullet k] + [(x \bullet k) \circ k]}{2} \quad (39)$$

where $k$ is a flat structuring element (zero line). The generation of a feature signal for the QRS complexes is accomplished by the operation

$$z = \tilde{x} - [(\tilde{x} \circ B) \bullet B] \quad (40)$$

where $B$ is now a peaky structuring element as shown in Fig. 9. In [114] $B$ has a length of 13 samples. A QRS complex is eventually found by comparing the feature signal against an adaptive threshold.

### Matched Filters

Besides the neural-network-based matched filtering approach in [122], there are linear matched filtering approaches as, for example, reported in [94, 27, 69, 25]. In [94], after some analog preprocessing steps such as an automatic gain control, the ECG signal is digitized and further processed by a comb filter (low pass) with a notch at 50 Hz and a bandpass filter with cut-off frequencies at 15 Hz and 40 Hz. This digital filter stage is followed by a matched filter for further improvement of the signal-to-noise ratio (SNR). The matched filtering is accomplished by

$$y(n) = \sum_{i=0}^{N-1} h(i) x(n-i) \quad (41)$$

where the impulse response $h(n)$ is the time-reversed template of the waveform to be detected. The impulse response of the matched filter $h(n)$ is manually taken from the first cardiac cycles of the current measurements; i.e., it needs to be determined interactively. For further enhancement of the timing accuracy, the output of the matched filter is interpolated up to four times the original sampling frequency. The final decision about a QRS complex is taken by comparing the filtered signal against a fixed threshold. It is reported in [94] that the matched filter also improves the timing accuracy of the detected R-wave.

A similar approach is proposed in [69]. Instead of computing the cross correlation between the template and the signal as in Eq. (41), the algorithm searches for the minimum of the *average magnitude cross difference* (AMCD)

| Table 1. Sets Used in Syntactic Approaches for ECG Event Detection. | | | | |
|---|---|---|---|---|
| | **Set (alphabet)** | **Primitives** | **Symbols** | **Reference** |
| (1) | $\Sigma = \{a,b,c\}$ | square of the first derivative $y_1^2$ | $a,b,c$ depend on amplitude and duration of peaks of $y_1^2$ | [9] |
| (2) | $\Sigma = \{(a,b) \mid a \in \{/,\backslash,0\}, b \in \{+,-,*\}\}$ | line segments | $a$: slope of the line segment, i.e. positive slope (/), negative slope (\) or zero slope (0). $b$: start point of the line segment, i.e. above (+), below (–) or on the baseline (*) | [46] |
| (3) | $\Sigma = \{h, s, s_n, i, i_n, l, l_n\}$ | line segments | horizontal ($h$), small ($s$), negative small ($s_n$), intermediate ($i$), negative intermediate ($i_n$), large ($l$) and negative large ($l_n$) slope | [117] |
| (4) | $\Sigma = \{(l_P,i,n),(s_P,i,n),(s_N,i,n),(l_N,i,n)\}$ | line segments | $\{l_P, s_P, s_N, l_N\}$: slope of line segment; $i,n$: time coordinate and duration of line segment (attribute values) | [87] |
| (5) | $\Sigma = \{K^+,K^-,E,\Pi\}$ | peak, line and parabolic segment | $K^+$ (positive peak), $K^-$ (negative peak), $E$ (line segment), $\Pi$ (parabolic segment), and additional attribute values describing the primitives. | [113] |

$$\mathrm{AMCD} = \sum_{i=1}^{N} |x(n-i) - h(i)| \tag{42}$$

where $x(n)$ is the ECG signal and $h(i)$ is the time-reversed template. This algorithm does not need multiplications and is therefore computationally inexpensive. In [69], templates of length $N = 10$ and $N = 20$ at a sampling frequency of 500 Hz are used. The ECG signal as well as the template need to be detrended before the calculation of the AMCD.

Further applications of matched filters are reported in [25] and [27], where integrated circuits are used for the real-time computation of the correlation coefficient and a wave digital filter realization is shown, respectively.

## Genetic Algorithms

In [91], genetic algorithms have been applied to a combined design of optimal polynomial filters for the preprocessing of the ECG and the parameters of a decision stage.

Polynomial filters are defined by [91]

$$y_n = \underbrace{\sum_{k_1=0}^{M}\sum_{k_2=0}^{M}\cdots\sum_{k_N=0}^{M}}_{\sum k_j \le M} a_{k_1 k_2 \cdots k_N} x_{n-d_1}^{k_1} x_{n-d_2}^{k_2} \cdots x_{n-d_N}^{k_N} \tag{43}$$

where the $d_j$ are delays with respect to the time $n$. Three different special cases of a polynomial filter are investigated: quasi-linear filters with consecutive samples ($M = 1$ and $N = 10$), quasi-linear filters with selected samples ($M = 1$ and $N = 5$), and quadratic filters with selected samples ($M = 2$ and $N = 3$).

The decision stage consists mainly of an adaptive threshold that is compared against the filtered ECG signal. The threshold adaption parameters are optimized in conjunction with the polynomial filter via a genetic optimization algorithm.

## Hilbert Transform-Based QRS Detection

In [124, 82] the use of the Hilbert transform for QRS detection is proposed. The Hilbert transform of a real signal $x$ is defined by

$$x_H(t) = \mathcal{H}\{x\} = \frac{1}{\pi}\int_{-\infty}^{\infty}\frac{x(\tau)}{t-\tau}d\tau = x_H(t) = x(t) * \frac{1}{\pi t} \tag{44}$$

and may be computed in the frequency domain as

$$X_H(j\omega) = X(j\omega)\cdot[-j\cdot\mathrm{sgn}(\omega)] = X(j\omega)\cdot H(j\omega) \tag{45}$$

where the transfer function of the Hilbert transform $H(j\omega)$ is given by

$$H(j\omega) = \begin{cases} -j & 0 \le \omega < \pi \\ j & -\pi \le \omega < 0. \end{cases} \tag{46}$$

Using the fast Fourier transform (FFT), the Hilbert transform can easily be computed. In [82] the ideal Hilbert transformator is approximated by a bandlimited $(2N+1)$-tap FIR filter with the impulse response $h(n)$. For example, the impulse response for the filter of the order $N = 11$ is given by [82]

$$h(n) = \{-0.038, 0, -0.143, 0, -0.610, 0, 0.610, 0, 0.143, 0, 0.038\}. \tag{47}$$

Impulse responses for other filter orders are listed in [82].

The Hilbert transform $x_H(n)$ of the ECG signal $x(n)$ is used for the computation of the signal envelope [82], which is given for bandlimited signals by

$$x_e(n) = \sqrt{x^2(n) + x_H^2(n)}. \tag{48}$$

A computationally less expensive approximation to the envelope can be made by [82]

$$x_e(n) \approx |x(n)| + |x_H(n)|. \tag{49}$$

In order to remove ripples from the envelope and to avoid ambiguities in the peak level detection, in [82] the envelope is low-pass filtered. Additionally, in [82] a waveform adaptive scheme for the removal of low frequency ECG components is proposed.

The method published in [124] is related to the algorithms based on the Hilbert transform. In [124] the envelope of the signal is approximated by

$$x_e(n) \approx |x_1(n)| + |x_2(n)| \tag{50}$$

where $x_1(n)$ and $x_2(n)$ are the outputs of two orthogonal digital filters; i.e.,

$$x_1(n) = x(n) - x(n-6) \text{ and} \tag{51}$$

$$x_2(n) = x(n) - x(n-2) - x(n-6) - x(n-8). \tag{52}$$

In order to remove noise, the envelope signal $x_e(n)$ is smoothed by a four-tap moving average filter.

### Length and Energy Transforms

In [36, 37] the application of *length* and *energy* transforms to QRS detection is investigated. The transforms are defined for multichannel ECG signals but may also be used for single-channel ECG analysis. They are given by

$$L(n,q,i) = \sum_{k=i}^{i+q-1} \sqrt{\sum_{j=1}^{n} (\Delta x_{j,k})^2}$$

length transform (53)

$$E(n,q,i) = \sum_{k=i}^{i+q-1} \sum_{j=1}^{n} (\Delta x_{j,k})^2$$

energy transform (54)

where $n$ is the number of ECG channels, $i$ is the time index, $q$ denotes the window length, and $\Delta x_{j,k} = x_{j,k} - x_{j,k-1}$. These formulas are based on the assumption that the derivatives of the ECG channels can be considered as the elements of a vector. The length of the vector is determined from the square root of the second sum in Eq. (53). The length transform represents a temporarily smoothed time course of the vector length. A similar assumption leads to the energy transform, which can be interpreted as the short-term energy estimation of the vector. The authors of [36, 37] state that both transforms are superior to conventional transforms for feature extraction, whereas the length transform works particularly good in cases of small QRS complexes.

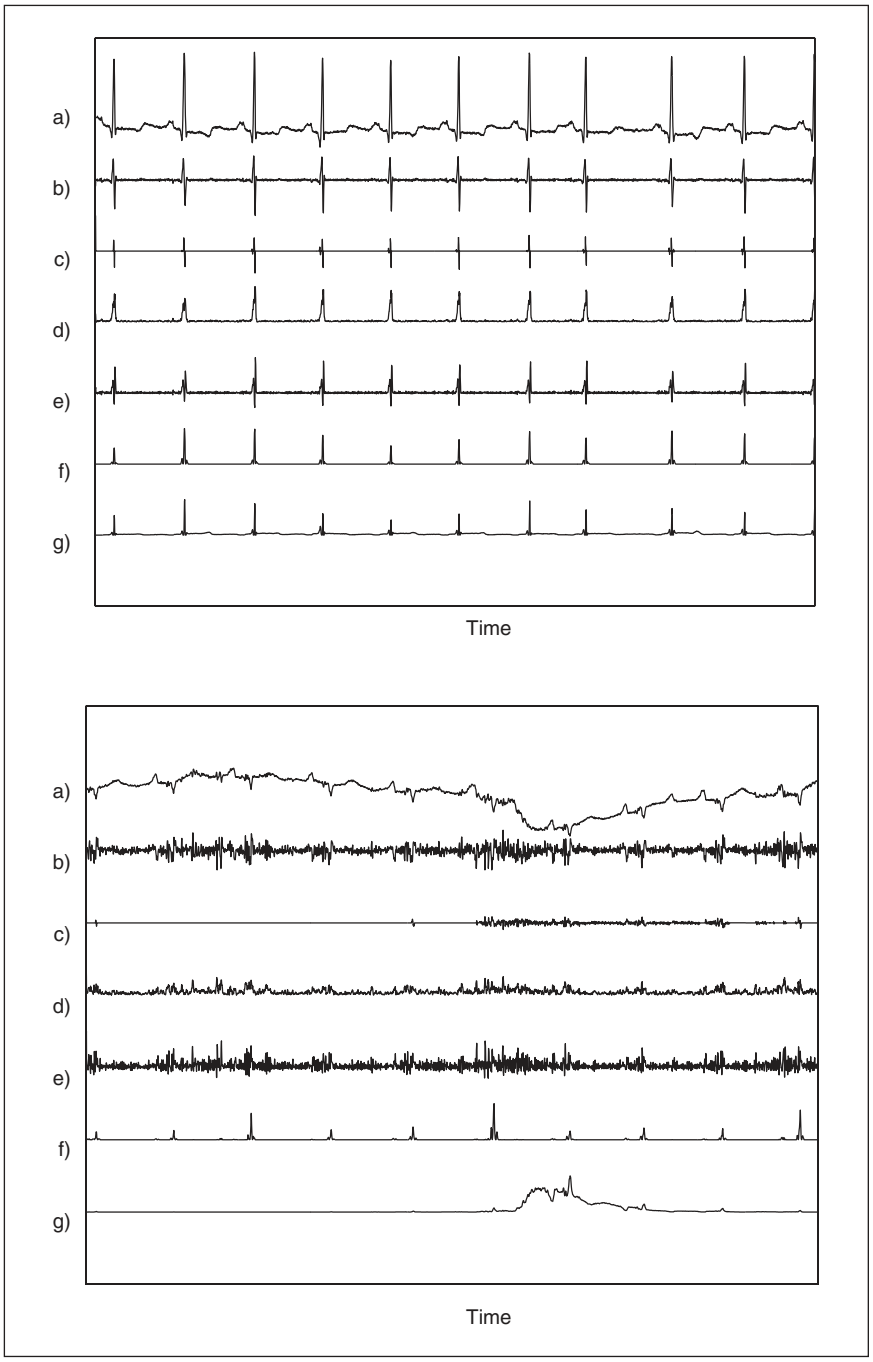


**10. (a) ECG signal (top: from record 100; bottom: from record 108), (b) first derivative from Eq. (1), (c) first derivative from Eq. (4), (d) feature from Eq. (8), (e) feature from Eq. (9), (f) feature from [83], (g) MOBD feature signal.**

### Syntactic Methods

Syntactic algorithms for ECG processing have been proposed in [9, 19, 86, 97, 113]. A review of several algorithms is given in [98]. The signal to be analyzed by a syntactic method is assumed to be a concatenation of linguistically represented primitive patterns; i.e., strings. Using a grammar, this string representation is parsed for strings coding a search pattern. Therefore, a syntatic algorithm for pattern recognition essentially requires the definition of primitive patterns, a suitable linguistic representation (alphabet) of the primitive patterns, and the formulation of a pattern grammar.

In ECG processing the signal is split into short segments of a variable or a fixed length. Each segment is then represented by a primitive and coded using the predefined alphabet. Due to their computational efficiency, most algorithms use line segments as primitives for the signal representation [9, 46, 87, 117]. In [113] the set of line primitives is extended by peaks, parabolic curves, and additional attributes. An overview of several primitive patterns, alphabets, and attributes is given in Table 1.

Various grammars for these alphabets (i.e., rules describing the set of search patterns) are proposed in [35, 46, 88, 87, 113, 115, 117].

### QRS Detection Based on MAP Estimation

*Maximum a posteriori* (MAP) estimation can be considered as a special case within the Bayesian framework, which provides a very general basis for parameter estimation including the incorporation of prior knowledge. The MAP estimate $\hat{\theta}_{MAP}$ of a parameter $\theta$ given the observation $\boldsymbol{x}$ is defined by

$$\hat{\theta}_{MAP} = \underset{\theta}{\operatorname{argmax}}\, f_{\theta}(\theta|\boldsymbol{x}) \quad (55)$$

where

$$f_\theta(\theta|\boldsymbol{x}) = \frac{f_x(\boldsymbol{x}|\theta) f_\theta(\theta)}{f_x(\boldsymbol{x})} \tag{56}$$

is the a posteriori probability density function (pdf) of $\theta$ given $\boldsymbol{x}$. The a priori pdf $f_\theta(\theta)$ of the parameter $\theta$ represents the available prior knowledge.

In [12] a QRS detection method based on MAP estimation is presented. The proposed model for the $N$-dimensional vector $\boldsymbol{x}$ of ECG samples is given by

$$x(n) = \begin{cases} \sum_{i=1}^{q} B_i s(n-\theta_i, T_i) + w(n) & : \ 1 \le q \le k \\ w(n) & : \ q = 0. \end{cases} \tag{57}$$

where $q$ is the number of *pulse-shaped* peaks $s(n, T)$ in the ECG segment and $\boldsymbol{x}$ and $k$ denote the number of *all* peaks in the same segment. $B_i$, $T_i$, and $\theta_i, i = 1 \ldots k$ give the amplitude, duration, and arrival time for the $i$-th peak, respectively. $w(n)$ is additive white Gaussian noise. For a given joint a priori pdf $f_{q,B,T,\theta}(q, \boldsymbol{B}, \boldsymbol{T}, \theta)$, the MAP estimate of the model parameters is given by

$$(\hat{q}, \hat{\boldsymbol{B}}, \hat{\boldsymbol{T}}, \hat{\theta}) = \underset{q, \boldsymbol{B}, \boldsymbol{T}, \theta}{\operatorname{argmax}} \ V(\boldsymbol{x}, q, \boldsymbol{B}, \boldsymbol{T}, \theta) \tag{58}$$

with $V(\boldsymbol{x}, q, \boldsymbol{B}, \boldsymbol{T}, \theta)$ being the log-likelihood function with respect to $f_{q,B,T,\theta}(q, \boldsymbol{B}, \boldsymbol{T}, \theta)$. Detailed considerations of the prior knowledge leading to a joint a priori pdf $f_{q,B,T,\theta}(q, \boldsymbol{B}, \boldsymbol{T}, \theta)$ are described in [12].

Since the maximization process is computationally expensive, the authors also present modifications for an approximate MAP estimation. Further simplifications are presented in [100].

### Zero-Crossing-Based QRS Detection

QRS detection based on zero crossing counts is proposed in [59]. After bandpass filtering, a high-frequency sequence $b(n) = k(n) \cdot (-1)^n$ is added to the filtered signal $y_1(n)$; i.e.,

$$y_2(n) = y_1(n) + b(n). \tag{59}$$

The amplitude of the high-frequency sequence $k(n)$ is determined from a running average of the modulus of the bandpass-filtered ECG $|y_1(n)|$. Since the amplitude of $k(n)$ is lower than the amplitude of the QRS complex, the number of zero crossings is large during non-QRS segments and low during the QRS complex. Computing a running average of the number of zero crossings results in a robust feature $z(n)$ for the QRS complexes. The feature signal $z(n)$ is compared against an adaptive threshold for the detection of QRS complexes. The temporal location of the R-wave is found by a maximum search in the bandpass-filtered signal around a detected QRS candidate.

## Benchmark Databases

Several standard ECG databases are available for the evaluation of software QRS detection algorithms. Tests on these well-annotated and validated databases provide reproducible and comparable results. Furthermore, these databases contain a large number of selected signals representative for the large variety of ECGs as well as signals that are rarely observed but clinically important.

Available standard databases include:

1) *MIT-BIH Database*

The MIT-BIH database [76] provided by MIT and Boston's Beth Israel Hospital

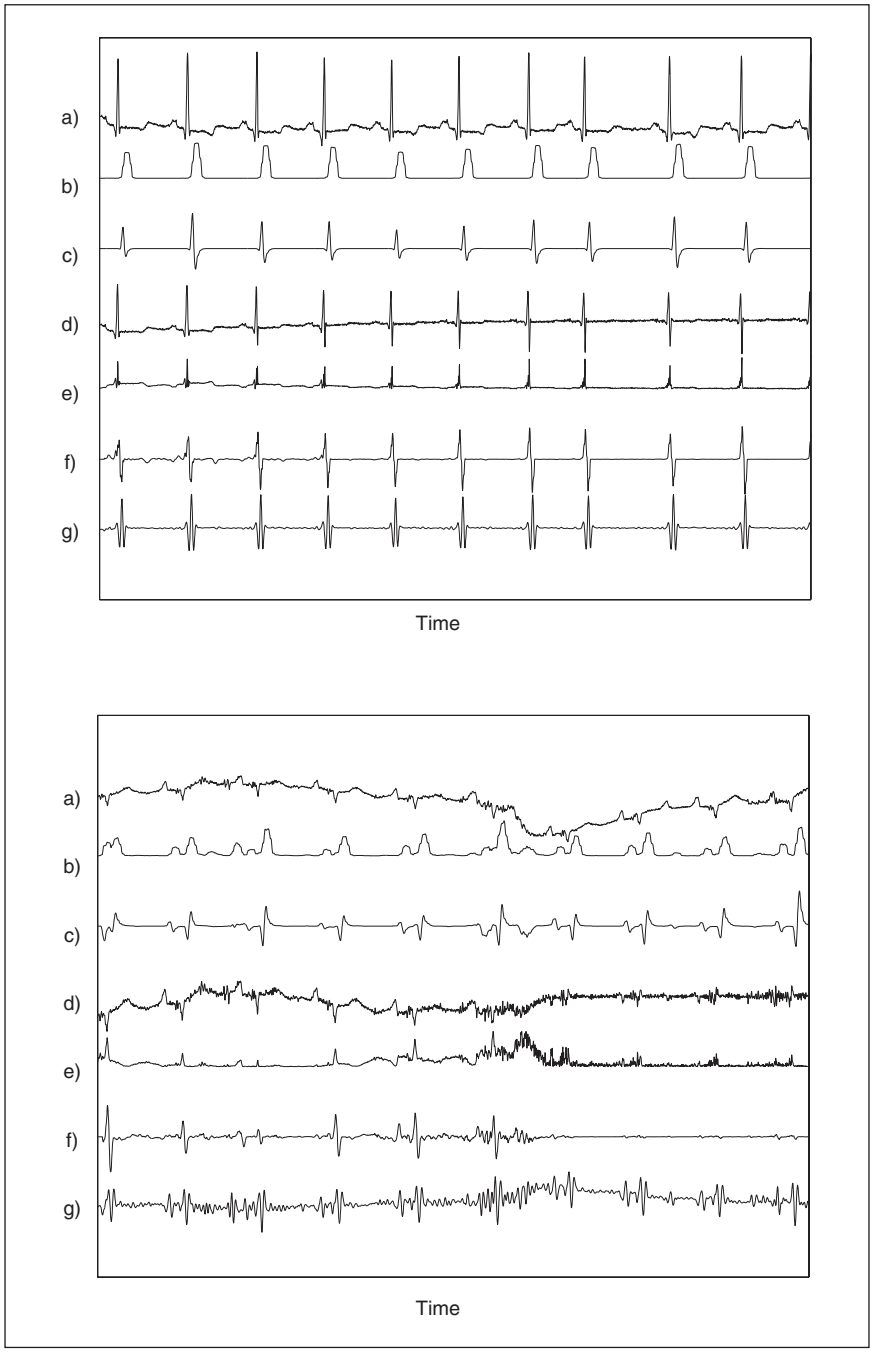


**11. (a) ECG signal (top: from record 100; bottom: from record 108), (b) Feature by [41], (c) feature by [26], (d) LMS prediction error $e(n)$ (filter order 2, step size $\lambda = 0.03$), (e) LMS feature from Eq. (34) (filter order 2, step size $\lambda = 0.03$), (f) LMS feature from Eq. (35) (filter order 2, step size $\lambda = 0.03$), (g) matched filter feature.**

consists of ten databases for various test purposes; i.e., the Arrhythmia Database, the Noise Stress Test Database, the Ventricular Tachyarrhythmia Database from Creighton University Cardiac Center, the ST Change Database, the Malignant Ventricular Arrhythmia Database, the Atrial Fibrillation/Flutter Database, the ECG Compression Test Database, the Supraventricular Arrhythmia Database, the Long-Term Database, and the Normal Sinus Rhythm Database. In addition to the AHA (see below) database and the European ST-T Database (see below), the first three MIT-BIH databases are required by the ANSI for testing ambulatory ECG devices.

Most frequently the MIT-BIH Arrhythmia Database is used. It contains 48 half-hour recordings of annotated ECG with a sampling rate of 360 Hz and 11-bit resolution over a 10-mV range. Twenty-five recordings (records number 200 and above) with less common arrhythmias were selected from over 4000 24-hour ambulatory ECG recordings, and the rest was chosen randomly. Altogether there are 116137 QRS complexes in this database. While some records contain clear R-peaks and few artifacts (e.g., records 100-107), for some records the detection of QRS complexes is very difficult due to abnormal shapes, noise, and artifacts (e.g., records 108 and 207).

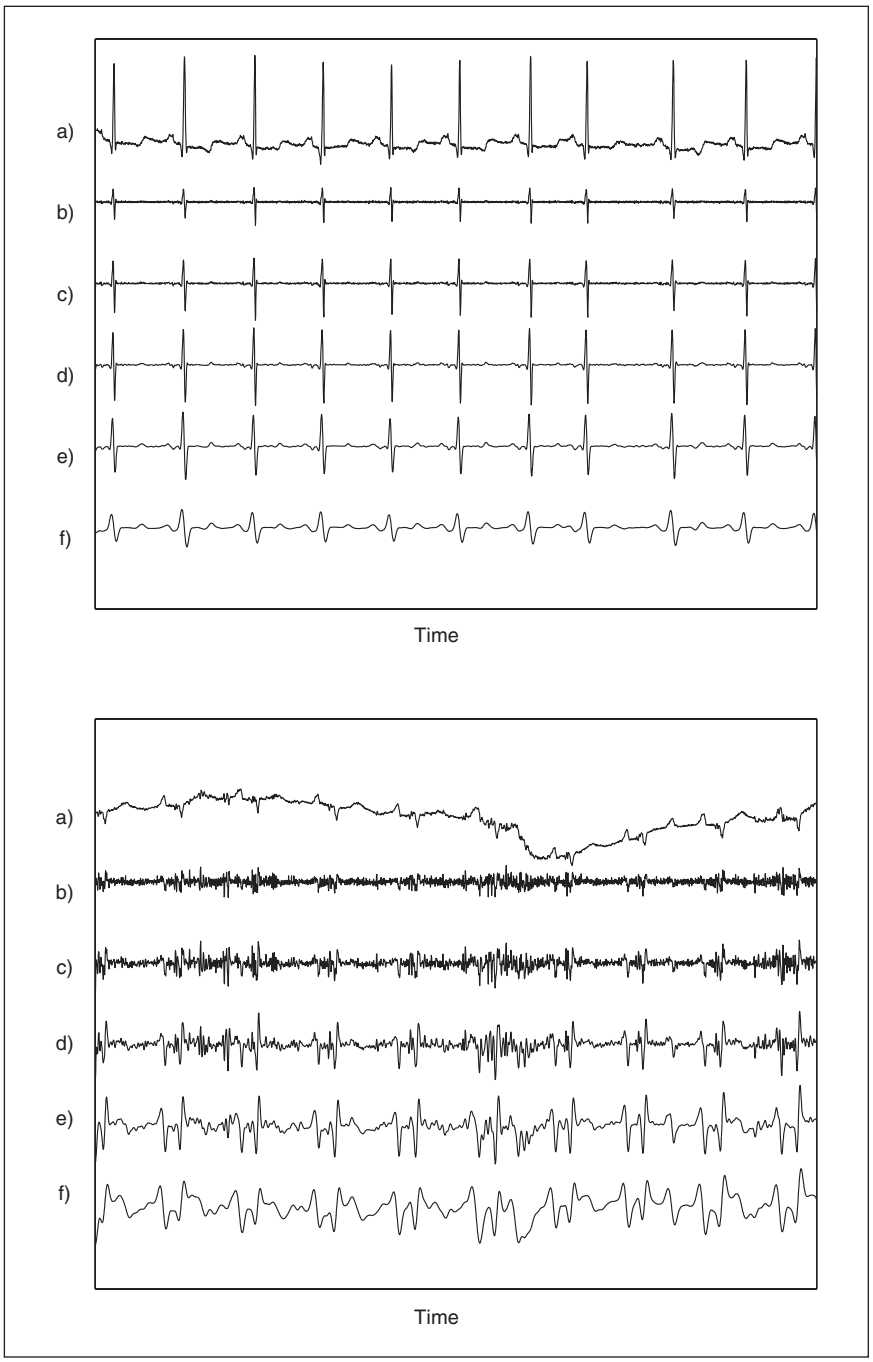


**12. (a) ECG signal (top: from record 100; bottom: from record 108); wavelet subband signals for the scales $j = 1$ (b) to $j = 5$ (f). For the wavelet transform the spline wavelet proposed in [74] was used.**

2) *AHA Database*

The AHA Database for Evaluation of Ventricular Arrhythmia Detectors [4] of the American Heart Association contains 155 recordings of ambulatory ECG. The signals have been digitized with a sampling rate of 250 Hz and a resolution of 12 bits over 20 mV. Each record consists of 2.5 hours of unannotated signal followed by 30 minutes of annotated ECG. The records are arranged into eight groups representing different levels of ectopic excitation. Records 1001 to 1020 of the first group show no extra systoles, whereas records 8001 to 8010 containing ECGs with ventricular fibrillation show the highest level of ventricular ectopy.

3) *Ann Arbor Electrogram Libraries*

The Ann Arbor Electrogram Libraries [52] are a collection of more than 800 intracardiac electrograms and surface ECGs. Each recording consists of intracardiac unipolar and bipolar electrocardiograms and a surface ECG. This database is especially valuable for the evaluation of algorithms for implantable cardiac devices.

4) *CSE Database*

The Common Standards for Electrocardiography (CSE) Database [10] is frequently used for the evaluation of diagnostic ECG analyzers. The CSE Database consists of about 1000 multilead recordings (12 or 15 leads).

5) *Other Standard Databases*

More libraries available for evaluation of detection and classification algorithms are the European ST-T Database [80], the QT Database [64], the MGH Database [75], the IMPROVE Data Library [120], and the ECG Reference Data Set [89] of the Physikalisch-Technische Bundesanstalt (PTB). The ST-T Database contains 90 recordings of two hours of ECG each, selected for the evaluation of ECG devices that analyze ST levels and T-waves. The QT Database was designed for evaluation of algorithms that detect waveform boundaries in the ECG. For this

database, 105 records with a broad variety of QRS and ST-T morphologies were selected from other databases; e.g., the MIT-BIH Arrhythmia Database and the European ST-T Database. Each record has a length of 15 minutes. The databases of the Massachusetts General Hospital and the IMPROVE database are multichannel recordings containing a three-lead ECG and additional signals such as systemic and pulmonary aterial pressure (SAP, PAP), central venous pressure (CVP), $CO_2$, $O_2$, and respiration. The ECG Reference Data Set of the PTB is not finished yet. Currently, this database contains more than 500 records with durations from 38 s to 120 s. The classification follows the classification scheme of the AHA.

## Evaluation and Comparison

The usage of software QRS detection algorithms in medical devices requires the evaluation of the detection performance. According to [1], essentially two parameters should be used to evaluate the algorithms; that is,

$$Se = \frac{TP}{TP + FN} \quad \text{sensitivity} \tag{60}$$

$$+P = \frac{TP}{TP + FP} \quad \text{positive predictivity} \tag{61}$$

where $TP$ denotes the number of true positive detections, $FN$ the number of false negatives, and $FP$ the number of false positives. Furthermore, to achieve comparable and reproducible results, the evaluation needs to be carried out on standard databases.

Contrary to the requirements of comparability and reproducibility, in practice there are many publications where no evaluation is reported at all, the evaluation has not been done using standard databases, or the performance indices are not compatible to the sensitivity and positive predictivity parameters. This effectively leads to incomparable results.

In order to make a comparison possible, we rank the reported results with respect to how they were obtained; i.e.,

- reliable results: the algorithm is tested against a standard database,
- less reliable results; the algorithm is tested against parts of a standard database, and
- unreliable results: the algorithm is tested against a nonstandard database.

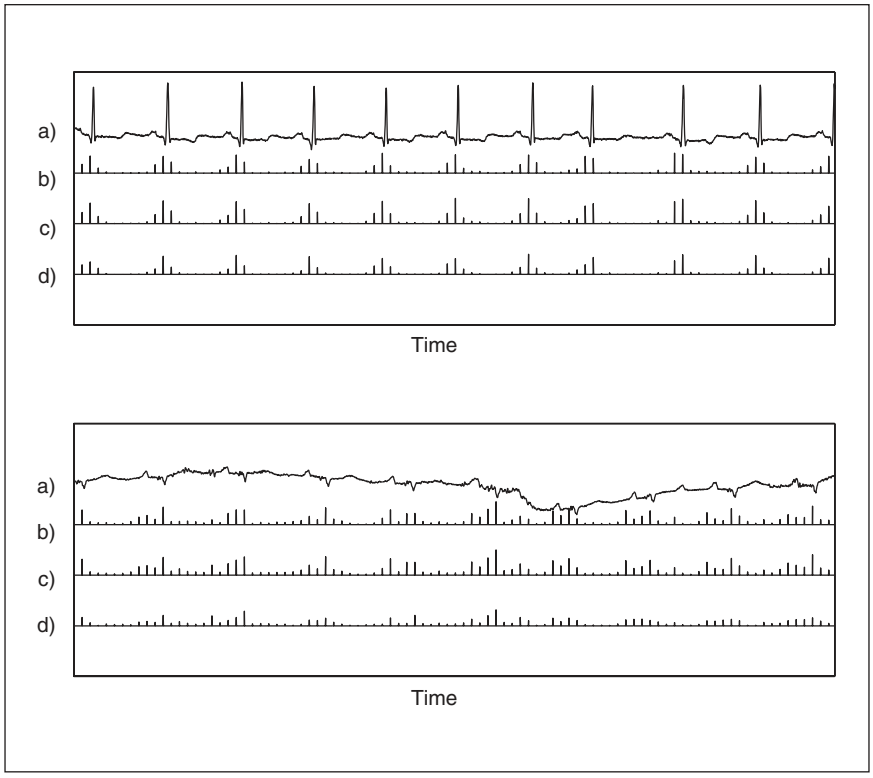


**13. Features of the filterbank approach [2], $M = 32$; (a) ECG signal (top: from record 100; bottom: from record 108), (b) feature signal $p_1$, (c) feature signal $p_2$, (d) feature signal $p_3$.**

Publications without reported or with incompatible results are not comparable and are not considered further. Results from the same reliability level are regarded as comparable. Within each reliability level the algorithms are grouped according to the reported performance.

The results of this comparison are shown in Table 1. It provides a quick overview of the achieved detection results and gives a good impression on what algorithms are potentially useful for an integration in larger ECG analysis systems. However, it should be clear that some simplifications have been made that need to be discussed. First of all, although some results are classified as less reliable or unreliable, nothing is said about the performance of the algorithm. Despite this reliability level, the actual algorithm may perform very well. In particular, in the case where only parts of a standard database have been used, the intention of the original authors frequently was to show the performance of the algorithm on particularly difficult records, such as records with pathological or very noisy signals. However, from an objective point of view, the reported results are not truly reliable, because the algorithm may have been tuned to perform perfectly on such pathological signals but not on the *normal* ECG. A further simplification is made by stating only the overall performance. That is, no statement is given on the worst case performance, which is also important. A third simplification is the disregard of the fact that the results may have been achieved by an extreme fine tuning of the parameters. In such cases the good reported results might be difficult to reproduce. Finally, this comparison discriminates against older algorithms, because in the early years of software QRS detection there were no standard databases available.

The algorithmic comparison with respect to the computational load can be carried out by grouping the algorithms into the categories low, medium, and high computational complexity. The comparison is shown in Table 2. Only the algorithms from Table 1 are considered. Again the grouping of the algorithms into these simple categories provides a quick overview, which is gained at the expense of lost information. In particular, for the comparison only the generation of the feature signals is considered. However, this limitation is reasonable since the feature generation is carried out for each sample of the ECG whereas the decision stage is

usually activated only a few times during a cardiac cycle. Furthermore, since the exact computational needs of these algorithms are not available, the algorithms are classified according to our experience. This simplification is of course subjective and not generally valid. However, in particular for researchers who are not familiar with QRS detection, this classification may give a general idea about the necessary processing power.

In order to give an impression about the difficulties in ECG analysis and QRS detection, some features of the presented algorithms are computed for two very different ECG segments. They are shown in Fig. 10 to Fig. 13. The signals are taken from records 100 and 108 of the MIT/BIH arrhythmia database. Whereas R-peaks in record 100 are very clear and easy to determine, the detection of QRS complexes is very difficult in record 108. Generally, detection problems may occur in case of

- noisy signals, electrode artifacts, baseline drift, power line interference;
- pathological signals;
- small QRS complexes; and
- sudden level changes of the QRS complex.

As can be seen from the figures, more sophisticated algorithms tend to cope better with these problems. Shortcomings of these features may be partly compensated for by suitable decision rules.

## Conclusions

The great variety of QRS detection algorithms presented in this review reflects the need for a reliable QRS detection in cardiac signal processing. Sensitivities and specificities of about 99.5% are possible for online QRS detectors today without much computational effort. These detection rates may be sufficient for clinical applications, whereas a higher performance may be necessary for research purposes. In that case, offline ECG analysis, where, for example, backsearch methods can be applied, may provide higher performance.

The currently achievable detection rates reflect only the overall performance of the detectors. These numbers hide the problems that are still present in case of noisy or pathological signals. A satisfying solution to these problems is still not found. However, recent advances in classification techniques such as novel softcomputing techniques have not been extensively transferred to the problem of QRS detection so that there are still many tools left for further improvements.

Many of the presented algorithms were not tested against a standard database or any database at all. This makes the results difficult to compare and to evaluate. With respect to the problems left in QRS detection, in particular the algorithmic behavior in case of noisy and pathological signals, only a comparable and reproducible evaluation on a standard database may show the progress achieved by a novel method.

*Bert-Uwe Köhler* received the Dipl.-Ing. degree and the Dr.-Ing. (Ph.D.) degree in electrical engineering from the Berlin University of Technology in 1995 and 1999, respectively. From 1995 until 2001 he worked as a researcher at the Department of Electrical Engineering of the Berlin University of Technology and gave courses in signal processing and medical electronics. In 2001, he joined the research and development department of

**Table 2. Comparison of the Results of Different Algorithms.**

| min[*S*,+*P*] | Standard Data Base | Parts of Standard Data Base | Nonstandard Data Base |
|---|---|---|---|
| > 99% | Afonso et al. [2],<br>Bahoura et al. [6],<br>Hamilton & Tompkins [41],<br>Inoue & Miyazaki [50],<br>Kohler et al. [59],<br>Li et al. [66],<br>Poli et al. [91] | Gritzali [36],<br>Hu et al. [47],<br>Kohama et al. [58],<br>Ruha et al. [94],<br>Sahambi et al. [95],<br>Vijaya et al. [119],<br>Xue et al. [122] | Belforte et al. [9],<br>Dobbs et al. [25],<br>Fischer et al. [32],<br>Thakor & Webster [109],<br>Yu et al. [123] |
| 95% - 99% | Suppappola & Sun [106][107] | Coast et al. [20],<br>Kadambe et al. [53][54] | Sörnmo et al. [100],<br>Udupa & Murthy [117] |
| 90% - 95% | | Papakonstantinou et al. [87],<br>Trahanias [114] | |
| < 90% | | | Ligtenberg & Kunt [67] |

**Table 3. Subjective Comparison with Respect to the Computational Load.**

| Low | Medium | High |
|---|---|---|
| Afonso et al. [2],<br>Fischer et al. [32],<br>Köhler et al. [59],<br>Kohama et al. [58],<br>Suppappola & Sun [106][107],<br>Trahanias [114],<br>Yu et al. [123] | Bahoura et al. [6],<br>Dobbs et al. [25],<br>Gritzali [36],<br>Hamilton & Tompkins [41],<br>Kadambe et al. [53][54],<br>Ligtenberg & Kunt [67],<br>Poli et al. [91],<br>Ruha et al. [94],<br>Vijaya et al. [119] | Belforte et al. [9],<br>Coast et al. [20],<br>Hu et al. [47],<br>Inoue & Miyazaki [50],<br>Li et al. [66],<br>Papakonstantinou et al. [87],<br>Sahambi et al. [95],<br>Sörnmo et al. [100],<br>Udupa & Murthy [117],<br>Xue et al. [122] |

Siemens Berlin. His research interests focus on statistical biomedical signal processing, in particular blind source separation and independent component analysis.

*Carsten Hennig* received the Dipl.-Ing. degree in electrical engineering from the Berlin University of Technology in 1999. From 1999 to 2001 he was working as a research assistant at the Berlin University of Technology. His research focuses on wavelet transform methods in digital signal processing and biomedical signal processing.

*Reinhold Orglmeister* received the Dipl.-Ing. degree and the Dr.-Ing. (Ph.D.) degree in electrical engineering from the Berlin University of Technology in 1980 and 1985, respectively. From 1980 to 1985 he worked on field theory at the Institute of Theoretical Electrical Engineering of the Berlin University of Technology. He was employed from 1985 until 1990 at the Berlin Research Institute of Robert Bosch GmbH, where he was responsible for digital signal processing. Since 1991 he has been a professor at the Department of Electrical Engineering at the Berlin University of Technology and since 2001 head of the Institute of Power Engineering and Automation. He teaches courses in signal processing, electronics, and medical electronics. His research interests include medical signal processing and microprocessor and DSP-based medical instrumentation.

**Address for Correspondence:** Reinhold Orglmeister, Berlin University of Technology, Department of Electrical Engineering, Biomedical Electronics Group, Einsteinufer 17/EN3, D-10587 Berlin, Germany. E-mail: orglmeister@tubife1.ee.tu-berlin.de.

## References

[1] *ANSI/AAMI EC57: Testing and reporting performance results of cardiac rhythm and ST segment measurement algorithms* (AAMI Recommended Practice/American National Standard), 1998. Available: http://www.aami.org; Order Code: EC57-293.

[2] V.X. Afonso, W.J. Tompkins, T.Q. Nguyen, and S. Luo, "ECG beat detection using filter banks," *IEEE Trans. Biomed. Eng.*, vol. 46, pp. 192-202, 1999.

[3] M.L. Ahlstrom and W.J. Tompkins, "Automated high-speed analysis of holter tapes with microcomputers," *IEEE Trans. Biomed. Eng.*, vol. 30, pp. 651-657, Oct. 1983.

[4] American Heart Association, AHA Database, ECRI, 5200 Butler Pike, Plymouth Meeting, PA 19462 USA.

[5] H. Baharestani, W.J. Tompkins, J.G. Webster, and R.B. Mazess, "Heart rate recorder," *Med. Biol. Eng. Comput.*, vol. 17, no. 6, pp. 719-723, Nov. 1979.

[6] M. Bahoura, M. Hassani, and M. Hubin, "DSP implementation of wavelet transform for real time ECG wave forms detection and heart rate analysis," *Comput. Methods Programs Biomed.*, vol. 52, no. 1, pp. 35-44, 1997.

[7] R.A. Balda, *Trends in Computer-Processed Electrocardiograms*. Amsterdam: North Holland, 1977, pp. 197-205.

[8] S. Barro, M. Fernandez-Delgado, J.A. Vila-Sobrino, C.V. Regueiro, and E. Sanchez, "Classifiying multichannel ECG patterns with an adaptive neural network," *IEEE Eng. Med. Biol. Mag.,* vol. 17, pp. 45-55, Jan./Feb. 1998.

[9] G. Belforte, R. De Mori, and F. Ferraris, "A contribution to the automatic processing of electrocardiograms using syntactic methods," *IEEE Trans. Biomed. Eng.*, vol. 26, pp. 125-136, Mar. 1979.

[10] J.H. van Bemmel and J.L. Williams, "Standardisation and validation of medical decision support systems: The CSE project," *Methods Inform. Med.*, vol. 29, pp. 261-262, 1990.

[11] C.M. Bishop and G. Hinton, *Neural Networks for Pattern Recognition*. New York: Clarendon Press, 1995.

[12] P.O. Börjesson, O. Pahlm, L. Sörnmo, and M.-E. Nygards, "Adaptive QRS detection based on maximum a posteriori estimation," *IEEE Trans. Biomed. Eng.*, vol. 29, pp. 341-351, May 1982.

[13] H.-H. Bothe, *Neuro-Fuzzy-Methoden*. Berlin, Germany: Springer-Verlag, 1997.

[14] C.S. Burrus, R.A. Gopinath, and H. Guo, *Introduction to Wavelets and Wavelet Transforms*. Upper Saddle River, NJ: Prentice Hall, 1998.

[15] G.G. Cano, S.A. Briller, and D.A. Coast, "Enhancement of low-level ECG components in noise with time-sequenced adaptive filtering," *J. Electrocardiology*, vol. 23 (Suppl.), pp. 176-183, 1990.

[16] B. Cellar, Y.C.C. Grace, and C. Phillips, "ECG analysis and processing using wavelets and other methods," *Biomed. Eng. Appl. Basis Commun.*, vol. 9, no. 2, pp. 81-90, 1997.

[17] I.I. Christov, I.A. Dotsinski, and I.K. Dasalkov, "High-pass filtering of ECG signals using QRS elemination," *Med. Biol. Eng. Comput.*, vol. 30, pp. 253-256, 1992.

[18] C.-H.H. Chu and E.J. Delp, "Impulsive noise suppression and background normalization of electrocardiogram signals using morphological operators," *IEEE Trans. Biomed. Eng.*, vol. 36, pp. 262-273, 1989.

[19] E.J. Ciaccio, S.M. Dunn, and M. Akay, "Biosignal pattern recognition and interpretation systems," *IEEE Eng. Med. Biol. Mag.*, pp. 269-273, 1994.

[20] D.A. Coast, R.M. Stern, G.G. Cano, and S.A. Briller, "An approach to cardiac arrhythmia analysis using hidden Markov models," *IEEE Trans. Biomed. Eng.*, vol. 37, pp. 826-836, 1990.

[21] J.A. Crowe, N.M. Gibson, M.S. Woolfson, and M.G. Somekh, "Wavelet transform as a potential tool for ECG analysis and compression," *J. Biomed. Eng.*, vol. 14, no. 3, pp. 268-272, 1992.

[22] S. Dandapat and G.C. Ray, "Spike detection in biomedical signals using midprediction filter," *Med. Biol. Eng. Comput.*, vol. 35, no. 4, pp. 354-360, 1997.

[23] I.K. Daskalov and I.I. Christov, "Electrocardiogram signal preprocessing for automatic detection of QRS boundaries," *Med. Eng. Phys.*, vol. 21, no. 1, pp. 37-44, 1999.

[24] V. Di-Virgilio, C. Francaiancia, S. Lino, and S. Cerutti, "ECG fiducial points detection through wavelet transform," in *1995 IEEE Eng. Med. Biol. 17th Ann. Conf. 21st Canadian Med. Biol. Eng. Conf.,* Montreal, Quebec, Canada, 1997, pp. 1051-1052.

[25] S. Dobbs, N. Schmitt, and H. Ozemek, "QRS detection by template matching using real-time correlation on a microcomputer," *J. Clin. Eng.*, vol. 9, no. 3, pp. 197-212, Sept. 1984.

[26] Z. Dokur, T. Olmez, E. Yazgan, and O.K. Ersoy, "Detection of ECG waveforms by neural networks," *Med. Eng. Phys.*, vol. 19, no. 8, pp. 738-741, 1997.

[27] D. Ebenezer and V. Krishnamurthy, "Wave digital matched filter for electrocardiogram preprocessing," *J. Biomed. Eng.*, vol. 15, no. 2, pp. 132-134, 1993.

[28] D. Ebenezer and F.F. Papa, "A recursive digital differentiator for ECG preprocessing," *Med. Eng. Phys.*, vol. 16, no. 4, pp. 273-277, 1994.

[29] W.A.H. Engelse and C. Zeelenberg, "A single scan algorithm for qrs-detection and feature extraction," in *IEEE Computers in Cardiology*. Long Beach, CA: IEEE Computer Society, 1979, pp. 37-42.

[30] T. Fancott and D.H. Wong, "A minicomputer system for direct high-speed analysis of cardiac arrhythmia in 24 h ambulatory ECG tape recordings," *IEEE Trans. Biomed. Eng.*, vol. 27, pp. 685-693, Dec. 1980.

[31] M. Fernandez-Delgado and S.B. Ameneiro, "MART: A multichannel ART-based neural network," *IEEE Trans. Neural Networks*, vol. 9, pp. 139-150, 1998.

[32] S.E. Fischer, S.A. Wickline, and C.H. Lorenz, "Novel real-time R-wave detection algorithm based on the vectorcardiogram for accurate gated magnetic resonance acquisitions," *Magn. Reson. Med.,* vol. 42, no. 2, pp. 361-70, 1999.

[33] J. Fraden and M.R. Neumann, "QRS wave detection," *Med. Biol. Eng. Comput.*, vol. 18, pp. 125-132, 1980.

[34] G.M. Friesen, T.C. Jannett, M.A. Jadallah, S.L. Yates, S.R. Quint, and H.T. Nagle, "A comparison of the noise sensitivity of nine QRS detection algorithms," *IEEE Trans. Biomed. Eng.*, vol. 37, pp. 85-98, 1990.

[35] K.S. Fu, "A step towards unification of syntactic and statistical pattern recognition," *IEEE Trans. Pattern Anal. Machine Intell.*, PAMI-5, pp. 200-205, Mar. 1983.

[36] F. Gritzali, "Towards a generalized scheme for QRS detection in ECG waveforms," *Signal Processing,* vol. 15, pp. 183-192, 1988.

[37] F. Gritzali, G. Frangakis, and G. Papakonstantinou, "A comparison of the length and energy transformations for the QRS detection," in *Proc. 9th Annu. Conf. IEEE Engineering in Medicine and Biology Society,* Boston, MA, 1987, pp. 549-550.

[38] D. Gustafson, "Automated VCG interpretation studies using signal analysis techniques," *R-1044 Charles Stark Draper Lab.*, Cambridge, MA, 1977.

[39] T.A. Gyaw and S.R. Ray, "The wavelet transform as a tool for recognition of biosignals," *Biomed. Sci. Instrum.*, vol. 30, pp. 63-68, 1994.

[40] F.M. Ham and S. Han, "Classification of cardiac arrhythmias using fuzzy ARTMAP," *IEEE Trans. Biomed. Eng.*, vol. 43, pp. 425-430, Apr. 1996.

[41] P.S. Hamilton and W.J. Tompkins, "Quantitative investigation of QRS detection rules using the MIT/BIH arrhythmiac database," *IEEE Trans. Biomed. Eng.*, vol. 33, pp. 1157-1165, 1986.

[42] P.S. Hamilton and W.J. Tompkins, "Adaptive matched filtering for QRS detection," in *Proc. Annu. Int. Conf. IEEE Engineering in Medicine and Biology Society,* New Orleans, LA, 1988, pp. 147-148.

[43] S. Haykin, *Adaptive Filter Theory,* 3rd ed. (Information and System Sciences Series). Englewood Cliffs, NJ: Prentice-Hall, 1996.

[44] S. Haykin, *Neural Networks, Comprehensive Foundation,* 2nd ed. Piscataway, NJ: IEEE Press, 1999.

[45] W.P. Holsinger, K.M. Kempner, and M.H. Miller, "A QRS preprocessor based on digital differentiation," *IEEE Trans. Biomed. Eng.*, vol. 18, pp. 121-217, May 1971.

[46] S.L. Horowitz, "A syntactic algorithm for peak detection in waveforms with appoications to cardiography," *Commun. ACM*, vol. 18, pp. 281-285, 1975.

[47] Y.H. Hu, W.J. Tompkins, J.L. Urrusti, and V.X. Afonso, "Applications of artificial neural networks for ECG signal detection and classification," *J. Electrocardiology*, vol. 26 (Suppl.), pp. 66-73, 1993.

[48] M. Hubelbank and C.L. Feldman, "A 60x computer-based Holter tape processing system," *Med. Instrum.,* vol. 12, no. 6, pp. 324-326, 1978.

[49] H. Inoue and A. Miyazaki, "A noise reduction method for ECG signals using the dyadic wavelet transform," in *1997 Int. Tech. Conf. Circuits/Systems, Computers and Communications (ITC-CSCC'97)*, Okinawa, Japan, 14-16 July 1997, *IEICE Trans. Fundamentals of Electron., Commun. Comput. Sci.*, E81-A, no. 6, pp. 1001-1007, 1998.

[50] H. Inoue, S. Iwasaki, M. Shimazu, and T. Katsura, "Detection of QRS complex in ECG using wavelet transform" (in Japanese), *IEICE Gen. Conf.*, vol. 67, no. A-4, p. 198, Mar. 1997.

[51] S. Jalaleddine and C. Hutchens, "Ambulatory ECG wave detection for automated analysis: A review," *ISA Trans.*, vol. 26, no. 4, pp. 33-43, 1987.

[52] J. Jenkins, Ann Arbor Electrogram Libraries, Available: http://electrogram.com/.

[53] S. Kadambe, R. Murray, and G.F. Boudreaux-Bartels, "The dyadic wavelet transform based QRS detector," in *1992 Conf. Rec. 26th Asilomar Conf. Signals, Systems and Computers,* vol. 1, pp. 130 -134.

[54] S. Kadambe, R. Murray, and G.F. Boudreaux-Bartels, "Wavelet transform-based QRS complex detector," *IEEE Trans. Biomed. Eng.*, vol. 46, pp. 838-848, 1999.

[55] L. Keselbrener, M. Keselbrener, and S. Akselrod, "Nonlinear high pass filter for R-wave detection in ECG signal," *Med. Eng. Phys.*, vol. 19, no. 5, pp. 481-484, 1997.

[56] L. Khadra, A.S. Al-Fahoum, and H. Al-Nashash, "Detection of life-threatening cardiac arrhythmias using the wavelet transformation," *Med. Biol. Eng. Comput.*, vol. 35, no. 6, pp. 626-632, 1997.

[57] K.S. Khobragade and R.B. Deshmukh, "ECG analysis using wavelet transforms," *IETE J. Res.*, vol. 43, no. 6, pp. 423-432, 1997.

[58] T. Kohama, S. Nakamura, and H. Hoshino, "An efficient R-R interval detection for ECG monitoring system," *IEICE Trans. Inf. Syst.*, E82-D, no. 10, pp. 1425-1432, Oct. 1999.

[59] B.-U. Köhler, C. Hennig, and R. Orglmeister, "QRS detection using zero crossing counts," submitted for publication, 2001.

[60] G. Kokturk, "A real-time simulated QRS detection system constructed using wavelet filtering technique," in *Proc. IEEE-SP Int. Symp. Time-Frequency and Time-Scale Analysis,* Pittsburgh, PA, 1998, pp. 281-284.

[61] A. Kyrkos, E. Giakoumakis, and G. Carayannis, "Time recursive prediction techniques on QRS detection problem," in *Proc. 9th Annu. Conf. IEEE Engineering in Medicine and Biology Society,* 13-16 Nov. 1987, Boston, MA, pp. 1885-1886.

[62] M. Lagerholm, C. Peterson, G. Braccini, L. Edenbrandt, and L. Soernmo, "Clustering ECG complexes using Hermite functions and self-organizing maps," *IEEE Trans. Biomed. Eng.*, vol. 47, pp. 838-848, 2000.

[63] P. Laguna, R. Jane, S. Olmos, N.V. Thakor, H. Rix, and P. Caminal, "Adaptive estimation of QRS complex wave features of ECG signal by the Hermite model," *Med. Biol. Eng. Comput.*, vol. 34, no. 1, pp. 58-68, 1996.

[64] P. Laguna, R.G. Mark, A. Goldberger, and G.B. Moody, "A database for evaluation of algorithms for measurement of QT and other waveform intervals in the ECG," *Comput. Cardiology*, vol. 24, pp. 673-676, 1997.

[65] J. Leski and E. Tkacz, "A new parallel concept for QRS complex detector," in *Proc. 14th Annu. Int. Conf. IEEE Engineering in Medicine and Biology Society,* Part 2, Paris, France, 1992, pp. 555-556.

[66] C. Li, C. Zheng, and C. Tai, "Detection of ECG characteristic points using wavelet transforms," *IEEE Trans. Biomed. Eng.*, vol. 42, pp. 21-28, 1995.

[67] A. Ligtenberg and M. Kunt, "A robust-digital QRS-detection algorithm for arrhythmia monitoring," *Comput. Biomed. Res.*, vol. 16, pp. 273-286, 1983.

[68] K.P. Lin and W.H. Chang, "QRS feature extraction using linear prediction," *IEEE Trans. Biomed. Eng.*, vol. 36, pp. 1050-1055, 1989.

[69] K.G. Lindecrantz and H. Lilja, "New software QRS detector algorithm suitable for real time application with low signal-to-noise ratios," *J. Biomed. Eng.*, vol. 10, no. 3, pp. 280-284, 1988.

[70] N. Maglaveras, T. Stamkopoulos, K. Diamantaras, C. Pappas, and M. Strintzis, "ECG pattern recognition and classification using non-linear transformations and neural networks: A review," *Int. J. Med. Informatics*, vol. 52, nos. 1-3, pp. 191-208, 1998.

[71] N. Maglaveras, T. Stamkopoulos, C. Pappas, and M. Strintzis, "ECG processing techniques based on neural networks and bidirectional associative memories," *J. Med. Eng. Technol.*, vol. 22, no. 3, pp. 106-111, 1998.

[72] N. Mahalingam and D. Kumar, "Neural networks for signal processing applications: ECG classification," *Australas. Phys. Eng. Sci. Med.*, vol. 20, no. 3, pp. 147-151, 1997.

[73] S. Mallat, "Zero-crossings of a wavelet-transform," *IEEE Trans. Inform. Theory*, vol. 37, pp. 1019-1033, 1991.

[74] S. Mallat and W.L. Hwang, "Singularity detection and processing with wavelets," *IEEE Trans. Inform. Theory,* vol. 38, pp. 617-643, 1992.

[75] Massachusetts General Hospital, Massachusetts General Hospital/Marquette Foundation Waveform Database, Dr. J. Cooper, MGH, Anesthesia Bioengineering Unit, Fruit Street, Boston, MA.

[76] Massachusetts Institute of Technology. MIT-BIH ECG database. Available: http://ecg.mit.edu/.

[77] C. May, N. Hubing, and A.W. Hahn, "Wavelet transforms for electrocardiogram processing," *Biomed. Sci. Instrum.,* vol. 33, pp. 1-6, 1997.

[78] P. Morizet-Mahoudeaux, C. Moreau, D. Moreau, and J.J. Quarante, "Simple microprocessor-based system for on-line ECG arrhythmia

analysis," *Med. Biol. Eng. Comput.*, vol. 19, no. 4, pp. 497-501, July 1981.

[79] W.C. Mueller, "Arrhythmia detection program for an ambulatory ECG monitor," *Biomed. Sci. Instrum.*, vol. 14, pp. 81-85, 1978.

[80] National Research Council (CNR). European ST-T Database. Institute of Clinical Physiology, Dept. of Bioengieering and Medical Informatics, Pisa, Italy. Available: http://www.ifc.pi.cnr.it/

[81] M.-E. Nygards and J. Hulting, "An automated system for ECG monitoring," *Comput. Biomed. Res.*, vol. 12, pp. 181-202, 1979.

[82] M.-E. Nygards and L. Sörnmo, "Delineation of the QRS complex using the envelope of the ECG," *Med. Biol. Eng. Comput.*, vol. 21, 1983.

[83] M. Okada, "A digital filter for the QRS complex detection," *IEEE Trans. Biomed. Eng.*, vol. 26, pp. 700-703, Dec. 1979.

[84] O. Pahlm and L. Sörnmo, "Software QRS detection in ambulatory monitoring—A review," *Med. Biol. Eng. Comput.*, vol. 22, pp. 289-297, 1984.

[85] J. Pan and W.J. Tompkins, "A real-time QRS detection algorithm," *IEEE Trans. Biomed. Eng.*, vol. 32, pp. 230-236, 1985.

[86] G. Papakonstantinou and F. Gritzali, "Syntactic filtering of ECG waveforms," *Comput. Biomed. Res.*, vol. 14, pp. 158-167, 1981.

[87] G. Papakonstantinou, E. Skordalakis, and F. Gritzali, "An attribute grammar for QRS detection," *Pattern Recognit.*, vol. 19, no. 4, pp. 297-303, 1986.

[88] G.K. Papakonstantinou, "An interpreter of attribute grammar and its application to waveform analysis," *IEEE Trans. Software Eng.*, SE-7, pp. 297-283, May 1981.

[89] Physikalisch-Technische Bundesanstalt. ECG Reference Data Set. Available: http://www.berlin.ptb.de/8/83/831/dbaccess/ecgrefdataset.html

[90] V. de Pinto, "Filters for the reduction of baseline wander and muscle artifact in the ECG," *J. Electrocardiology*, vol. 25 (Suppl.), pp. 40-48, 1992.

[91] R. Poli, S. Cagnoni, and G. Valli, "Genetic design of optimum linear and nonlinear QRS detectors," *IEEE Trans. Biomed. Eng.*, vol. 42, pp. 1137-1141, 1995.

[92] L.R. Rabiner, "A tutorial on hidden Markov models and selected applications in speech recognition," *Proc. IEEE,* vol. 77, pp. 257-286, Feb. 1989.

[93] K.D. Rao, "Dwt based detection of R-peaks and data compression of ECG signals," *IETE J. Res.*, vol. 43, no. 5, pp. 345-349, 1997.

[94] A. Ruha, S. Sallinen, and S. Nissila, "A real-time microprocessor QRS detector system with a 1-ms timing accuracy for the measurement of ambulatory HRV," *IEEE Trans. Biomed. Eng.*, vol. 44, pp. 159-167, 1997.

[95] J.S. Sahambi, S.N. Tandon, and R.K.P. Bhatt, "Using wavelet transforms for ECG characterization. An on-line digital signal processing system," *IEEE Eng. Med. Biol. Mag.*, vol. 16, pp. 77-83, 1997.

[96] L. Senhadji, J.J. Bellanger, G. Carrault, and J.L. Goatrieux, "Wavelet analysis of ECG signals," *Annu. Conf. IEEE Engineering in Medicine and Biology Society*, vol. 12, pp. 811-812, 1990.

[97] E. Skordalakis, "Recognition of noisy peaks in ECG waveforms," *Comput. Biomed. Res.*, vol. 17, pp. 208-221, 1984.

[98] E. Skordalakis, "Syntactic ECG processing: A review," *Pattern Recognit.*, vol. 19, no. 4, pp. 305-313, 1986.

[99] L. Sörnmo, "Time-varying digital filtering of ECG baseline wander," *Med. Biol. Eng. Comput.*, vol. 31, no. 5, pp. 503-508, 1993.

[100] L. Sörnmo, O. Pahlm, and M.-E. Nygards, "Adaptive QRS detection: A study of performance," *IEEE Trans. Biomed. Eng.*, BME-32, pp. 392-401, June 1985.

[101] L. Sörnmo, O. Pahlm, and M.E. Nygards, "Adaptive QRS detection in ambulatory ECG monitoring: A study of performance," in *Computers in Cardiology*. Long Beach, CA: IEEE Computer Society, 1982, pp. 201-204.

[102] A.L. Spitz and D.C. Harrison, "Automated family classification in ambulatory arrhythmia monitoring," *Med. Instrum.*, vol. 12, no. 6, pp. 322-323, 1978.

[103] C.A. Steinberg, S. Abraham, and C.A. Caceres, "Pattern recognition in the clinical electrocardiogram," *ISA Trans. Biomed. Electron.*, pp. 23-30, 1962.

[104] G. Strang and T. Nguyen, *Wavelets and Filter Banks*. Cambridge, MA: Wellesley-Cambridge Press, 1996.

[105] M.G. Strintzis, G. Stalidis, X. Magnisalis, and N. Maglaveras, "Use of neural networks for electrocardiogram (ECG) feature extraction, recognition and classification," *Neural Netw. World*, vol. 3, no. 4, pp. 313-327, 1992.

[106] Y. Sun, S. Suppappola, and T.A. Wrublewski, "Microcontroller-based real-time QRS detection," *Biomed. Instrum. Technol.*, vol. 26, no. 6, pp. 477-484, 1992.

[107] S. Suppappola and Y. Sun, "Nonlinear transforms of ECG signals for digital QRS detection: A quantitative analysis," *IEEE Trans. Biomed. Eng.*, vol. 41, pp. 397-400, 1994.

[108] Y. Suzuki, "Self-organizing QRS-wave recognition in ECG using neural networks," *IEEE Trans. Neural Networks*, vol. 6, pp. 1469-1477, 1995.

[109] N.V. Thakor and J.G. Webster, "Design and evaluation of QRS and noise detectors for ambulatory e.c.g. monitors," *Med. Biol. Eng. Comput.*, vol. 20, no. 6, pp. 709-714, 1982.

[110] N.V. Thakor, "Reliable R-wave detection from ambulatory subjects," *Biomed. Sci. Instrum.*, vol. 14, pp. 67-72, 1978.

[111] W.J. Tompkins, "An approach for physiological signal processing by laboratory minicomputer," *Comput. Programs Biomed.*, vol. 8, no. 1, pp. 16-28, 1978.

[112] W.J. Tompkins, "A portable microcomputer-based system for biomedical applications," *Biomed. Sci. Instrum.*, vol. 14, pp. 61-66, 1978.

[113] P. Trahanias and E. Skordalakis, "Syntactic pattern recognition of the ECG," *IEEE Trans. Pattern Anal. Machine Intell.*, vol. 12, pp. 648-657, 1990.

[114] P.E. Trahanias, "An approach to QRS complex detection using mathematical morphology," *IEEE Trans. Biomed. Eng.*, vol. 40, no. 2, pp. 201-205, 1993.

[115] W.-H. Tsai and K.-S. Fu, "Attributed grammar—A tool for combining syntactic and statistical approaches to pattern recognition," *IEEE Trans. Syst., Man, and Cybern.*, SMC-10, pp. 873-885, 1980.

[116] F.B. Tuteur, "Wavelet transformations in signal detection," in *Proc. ICASSP 88: 1988 Int. Conf. Acoustics, Speech, and Signal Processing,* New York, NY, 1988, pp. 1435-1438.

[117] J.K. Udupa and I. Murthy, "Syntactin approach to ECG rhythm analysis," *IEEE Trans. Biomed. Eng.*, BME-27, pp. 370-375, July 1980.

[118] S.V. Vaseghi, *Advanced Signal Processing and Digital Noise Reduction*. Wiley-Teubner, 1996.

[119] G. Vijaya, V. Kumar, and H.K. Verma, "ANN-based QRS-complex analysis of ECG," *J. Med. Eng. Technol.*, vol. 22, no. 4, pp. 160-167, 1998.

[120] VTT Technical Research Center of Finland. IMPROVE Data Library. Available: http://www.vtt.fi/tte/samba/projects/improve/

[121] J.G. Webster, "An intelligent monitor for ambulatory ECGs," *Biomed. Sci. Instrum.*, vol. 14, pp. 55-60, 1978.

[122] Q. Xue, Y. H. Hu, and W. J. Tompkins, "Neural-network-based adaptive matched filtering for QRS detection," *IEEE Trans. Biomed. Eng.*, vol. 39, pp. 317-329, 1992.

[123] B.C. Yu, S. Liu, M. Lee, C.Y. Chen, and B.N. Chiang, "A nonlinear digital filter for cardiac QRS complex detection," *J. Clin. Eng.*, vol. 10, pp. 193-201, 1985.

[124] S.-K. Zhou, J.-T. Wang, and J.-R. Xu, "The real-time detection of QRS-complex using the envelop of ECG," in *Proc. 10th Annu. Int. Conf., IEEE Engineering in Medicine and Biology Society,* New Orleans, LA, 1988, p. 38.